ELECTRO-MECHANICAL CHARACTERIZATION OF CHOLESTEROL – PHOSPHOLIPIDS INTERACTIONS IN DROPLET INTERFACE BILAYERS

By

JOYCE EL BEYROUTHY

(Under the Direction of Eric Freeman)

ABSTRACT

Droplet interface bilayers (DIB) allow for the creation of model cellular membranes at the interface of aqueous droplets dispersed in oil with dissolved phospholipids. Work in literature has shown that cholesterol greatly influences the mechanical properties of lipid membranes. However, little work has been done on studying cholesterol interaction with saturated phospholipids, particularly in DIB systems. **In this work, we investigate the electro-mechanical effects of cholesterol inclusion in lipid bilayers with DPhPC phospholipids, using DIBs as a platform.** First, the monolayer tension of the oil-water interface with lipids is measured using pendant drop tensiometry. It is then combined with the observed contact angle of the adhered droplets to estimate the energy-per-area of the film. This provides an estimation of the favorability of membrane formation through the energy of adhesion. Second, values for the critical dielectric stress are estimated and the influence of cholesterol on DIB durability is tracked.

INDEX WORDS: Lipid membrane, Cholesterol, Droplet interface bilayers, phospholipids, surface tension.

ELECTRO-MECHANICAL CHARACTERIZATION OF CHOLESTEROL – PHOSPHOLIPIDS INTERACTIONS IN DROPLET INTERFACE BILAYERS

By

JOYCE EL BEYROUTHY

B.E., Lebanese American University, Lebanon, 2016

A THESIS Submitted to the Graduate Faculty of The University of Georgia in Partial Fulfillment of the Requirements for the Degree

MASTER OF SCIENCE

Athens, GA

2018

ELECTRO-MECHANICAL CHARACTERIZATION OF CHOLESTEROL – PHOSPHOLIPIDS INTERACTIONS IN DROPLET INTERFACE BILAYERS

By

JOYCE EL BEYROUTHY

Major Professor: Eric Freeman

Committee: Donald Leo

Leidong Mao

Electronic Version Approved:

Suzanne Barbour

Dean of the Graduate School

The University of Georgia

May 2018

Table of Contents

List of Figures

Chapter 1: Introduction and Literature Review

Biological Cell Membranes

Cellular organisms are surrounded by a protective cell membrane, which is a semi-permeable barrier separating the cytoplasm from its surrounding environment [1]. It controls the diffusion and exchange of contents between the cell and the surrounding fluid. The membrane is consisted primarily of a double layer of phospholipids, or a lipid bilayer membrane [2]. However, multiple other molecules, such as proteins and cholesterol, are also found in the membrane depending on the cell's role and capabilities (Fig. 1). For instance, in the eye's cell membranes, cholesterol is present at a specific percentage to optimize light scattering [3].

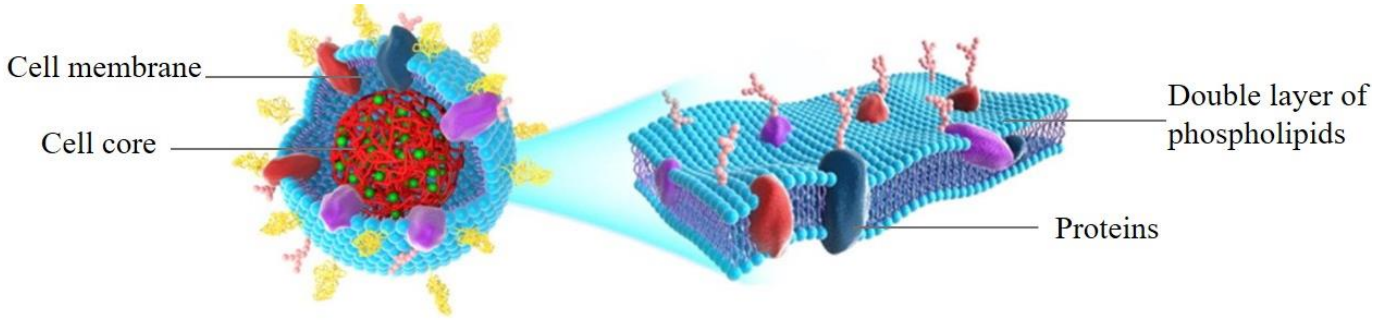

Figure 1: Cell membrane separating the cytoplasm from the extracellular fluid. The main structure is a double layer of phospholipids. However, proteins, cholesterol and other molecules can be found in the membrane depending on the cell's role[4].

Most plasma membranes in the human body are asymmetric [5] (Fig. 2). An asymmetric membrane is a membrane that shows an inconsistency or irregularity in between the leaflets composition. This characteristic is essential to the cell's growth and critical in determining its functionalities [5]. Asymmetry can be the result of a dissimilarity in the lipids composition. Kidney cells, for instance, have positively charged phospholipids in the exoplasmic – outer – leaflet, and

negatively charged or neutral phospholipids in the cytosolic – inner – leaflet [5]. This asymmetry is essential to the growth of these cells, distinctly. Another example of asymmetry is proteins' positions [6]. The same protein may be oriented inwards to a certain percentage in the membrane and outwards for the rest. This allows for separate chemical reactions inside and outside of the cell controlling its behavior and composition.

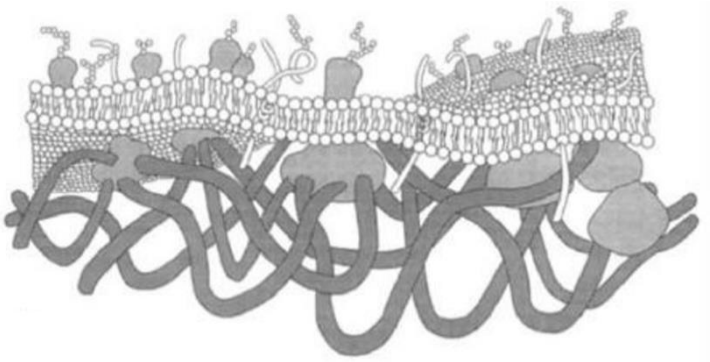

Figure 2: Red cell membrane model. The thick cytosolic compared to the thinner exoplasmic leaflet controls the functions and mass transfer across the bilayer [7].

Phospholipids

As mentioned earlier, the membrane is a double layer of phospholipids. Phospholipids are a special kind of lipids that incorporate a phosphate group. They are amphiphilic in nature as they contain a hydrophilic head and two hydrophobic tails [8] (Fig. 3). They can be charged or neutral, depending on the structure of the head group. They are also either saturated or unsaturated, depending on the carbon bonds in the hydrophobic tails. If all carbon bonds are single bonds, the fatty acid chains are saturated. Whereas, if there is at least one double bond in the tails, the molecule becomes unsaturated [9]. The saturation condition of phospholipids in the membrane highly impacts its physical state (Fig. 4). Unsaturated phospholipids lead to a more liquid-disordered membrane [10]. The double bonds or joints within the hydrophobic tails allow them to move freely, and form gaps

in between the molecules leading to a less packed and more permeable membrane. The higher the degree of unsaturation – number of double bonds in the hydrocarbon tails – the higher the disorder [11].

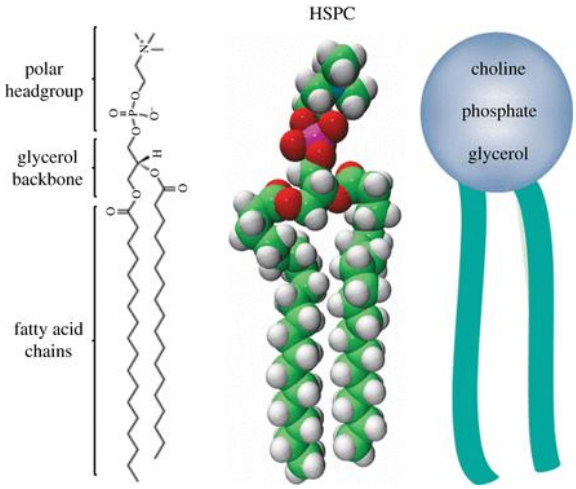

Figure 3: Phospholipid molecule, an amphiphilic structure having a hydrophilic head and two hydrophobic carbon chains – fatty acids [12].

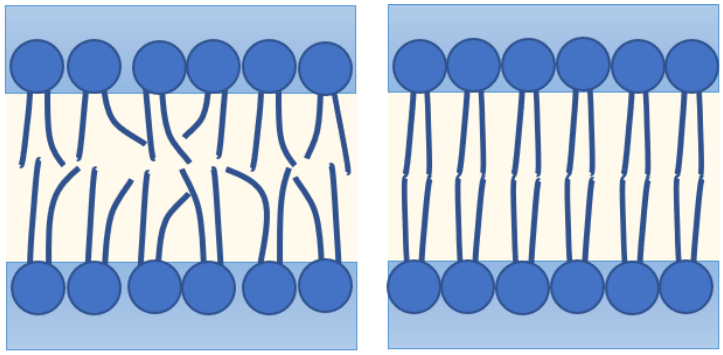

Figure 4: Fluidity of the lipid membrane depending on the phospholipids used. a) Unsaturated phospholipids lead to a more fluid-like bilayer as the carbon double bonds create an untidy fatty acid chains. b) Saturated fatty acid chains generate a relatively more ordered, gel-like membranes.

Model Membranes

Biological cell membranes have inspired scientists from a variety of fields due to their unique properties and behavior. Researchers are mimicking cell membranes for inter-disciplinary purposes. Work in literature shows that these synthetic membranes can be used for a diversity of purposes including drug delivery [13-16] and biosensing applications [17, 18]. Several methods have been developed in the last few decades to create synthetic lipid membranes. All of them are based on the amphiphilic property of lipids and on the presence of a polar and an apolar medium, which can be fluidic and/or solid. In the following paragraphs, some of the most influential techniques developed for forming synthetic lipid bilayers will be shortly described.

Montal-Mueller (MM) Technique

The Montal-Mueller technique, also known as lipids folding, is one of the earliest methods developed for model membranes in 1970s [19]. It is based on having a hydrophobic septum, usually made from Teflon or silicone, separating two electrolyte solutions. Phospholipids, which are primarily dissolved in chloroform or ethanol, are spread at the electrolyte surface forming the monolayer across the water-air interface. The bilayer is then created by raising the level of the electrolyte solutions simultaneously leading to the folding of the two monolayers at the septum level (Fig. 5). One of the main advantages of this technique is that the resulting bilayer is solvent free, as the chloroform or ethanol that would be used to spread the phospholipids on top of the electrolyte solutions is insured to evaporate after a relatively short amount of time [20].

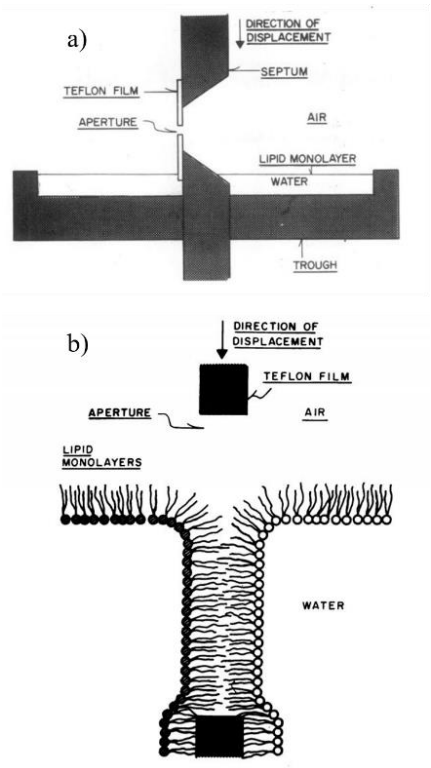

Figure 5: Montal-Mueller or the lipid folding technique [19]. a) Apparatus used to create the lipid bilayer: two electrolyte solutions separated by a hydrophobic septum, lipid monolayers are formed at the water-air interface. b) Increasing the electrolytes level with respect to the septum leads to the folding of the monolayers and the formation of a lipid bilayer.

Vesicle Fusion

Inspired from the behavior of eukaryote cells, the vesicle fusion technique relies on first, forming lipid vesicles in an aqueous medium, and second, driving them to a solid substrate, such as mica, glass or gold, where vesicle rupture occurs leading to the adhesion of the bilayer on the solid's surface [21] (Fig. 6). Vesicles are formed by first dissolving the lipids into an organic solvent such as chloroform and the solvent is then evaporated leaving a dry lipid film. The latter is hydrated with an aqueous buffer solution leading to the spontaneous vesicles formation. Vesicles' shape and size are controlled by a variety of sonication conditions – power and time [22]. Another usage of this technique is proteins incorporation into an existing bilayer. Phospholipids and the desired

proteins would be dissolved into the organic solvent and then rehydrated, as described earlier. Proteins incorporated vesicles merge with the pre-existing bilayer facilitating protein reconstitution [23].

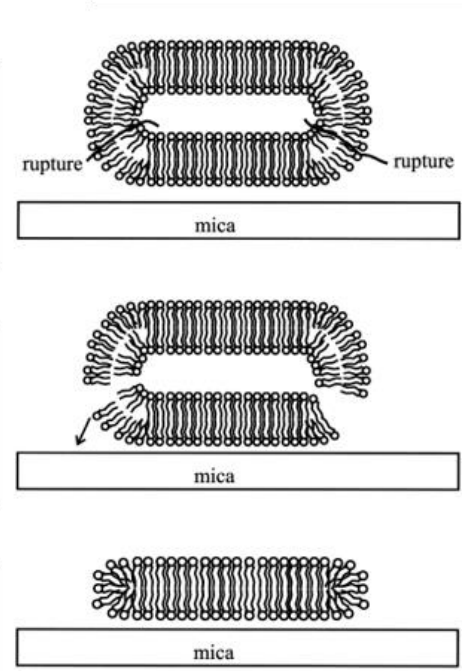

Figure 6: Vesicle fusion technique [21]. Lipid vesicles are formed and then driven to an adhering substrate where the bilayer is formed or to a pre-existing bilayer to facilitate protein insertion.

Lipid Painting

Lipid painting is one of the simplest techniques developed for model membranes [1]. It consists of a simple 3 step procedure (Fig.7). First, lipids dissolved in an organic solvent such as chloroform, are spread over a hydrophilic surface. Second, the solvent evaporates in few minutes leaving a dry film of lipids on the substrate. Finally, an aqueous solution is added on top of the substrate to rehydrate the lipids and the bilayer is formed as the system tries to minimize the free energy driven by hydrophobic interactions. However, this method has drawbacks. If any solvent

is left in the membrane, bilayer thinning, instability and protein denaturization can easily occur [20, 24].

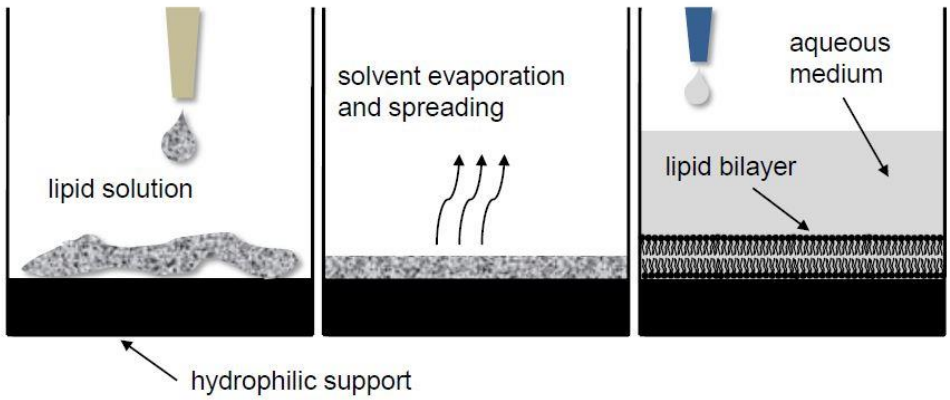

Figure 7: Lipid painting method [1]. Step 1: Lipids dissolved in an organic solvent spread on a hydrophilic surface. Step 2: Solvent evaporates leaving a dry film on the surface. Step 3: Hydrating the surface by means of a buffer aqueous solution, leading to the spontaneous formation of a lipid bilayer.

Droplet on Hydrogel Bilayer

Droplet on hydrogel bilayer (DHB) technique involves a solid hydrogel surface, an aqueous droplet and an apolar medium, such as oil (Fig. 8). An aqueous droplet is suspended from an electrode into the oil medium. Phospholipids are dissolved in oil leading to monolayer formation on both the hydrogel – oil interface as well as on the water – oil interface. The bilayer is then formed when the droplet is moved downwards, enabling it to sit on the hydrogel surface and the hydrophobic tails couple together expelling most of the oil out [1]. DHBs are stable as they were seen to last for weeks [25]. They are relatively easy to form and enable various configuration of single bilayers. However, asymmetric membranes remain a challenge [1].

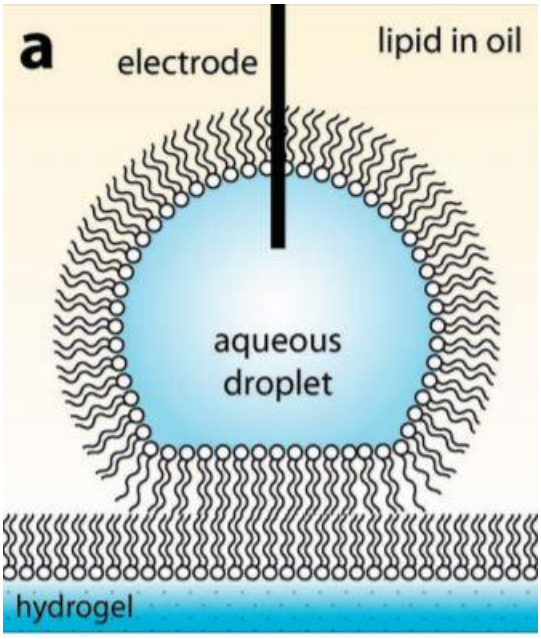

Figure 8: Droplet on hydrogel bilayer [26]. The bilayer is the coupling of hydrogel-oil and water-oil monolayers.

Chapter 2: Droplet Interface Bilayer Technique

The techniques discussed so far include at least one solid component for the system to sit on, reducing membrane's flexibility and restricting it by geometrical boundary conditions. The method that will be described next, the droplet interface bilayer (DIB), is established out of a purely fluidic system. The DIB technique will be the platform of this thesis work due to its fluidic nature, which enables a flexible control over the bilayer's geometry and provides a wide study of its electro-mechanical properties [27]. By studying DIBs, membrane's mechanics can be related back to droplets mechanics expanding the field of investigation and potential usage of lipid membranes.

The droplet interface bilayer is a technique developed in the early years of this century as the result of the combined efforts of David Needham [18], Kei Funakoshi [28], Jerome Bibette [29] and others, as a direct method for forming synthetic lipid membranes. The DIB method has gained popularity among researchers due to its multiple advantages and unique structure compared to alternative methods for model membrane formation. DIBs are relatively easy to make, durable, entirely fluidic, and able to be separated and reformed as needed.

This technique, similarly to other membrane forming techniques, relies on the amphiphilic property of lipids. The DIB technique submerges aqueous droplets made from a buffer solution in an apolar medium, usually oil. This allows for the self-assembly of lipid monolayers at the oil-water interface. The droplets are often suspended from a silver/silver-chloride electrodes which are tipped in agarose to aid in droplet adhesion (Fig.9) and allow for electrical characterization of the adhered interface. The lipid surfactants can be present either in the aqueous phase, lipids-in scenario, or in the oil phase, lipids-out. In both cases, phospholipids align on the water-oil interface

forming the monolayer. Monolayer stabilization takes a few minutes, and highly depends on where the phospholipids are dissolved and the type of oil used [30]. By simply bringing the two droplets together, the hydrophobic tails "zip" together forming a lipid bilayer membrane. At the micro-level, the droplets can be seen approaching each other and adhering until equilibrium is reached (Fig.10).

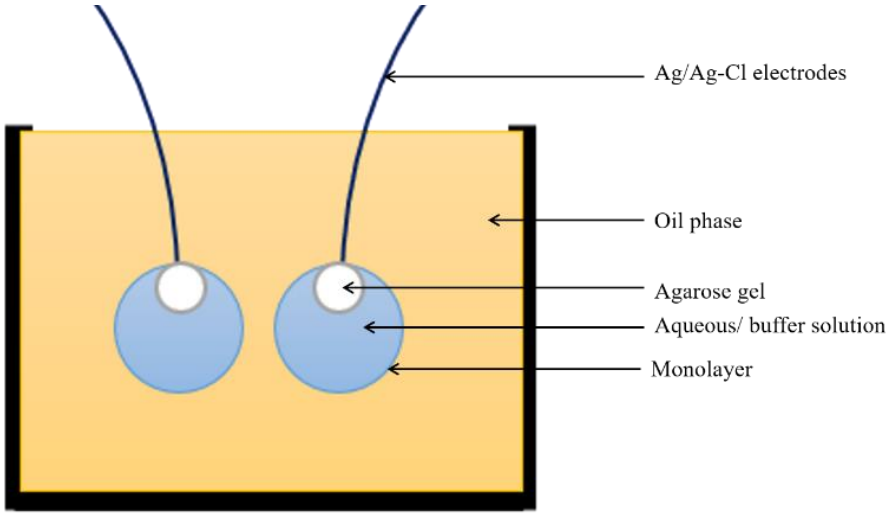

Figure 9: Droplet interface bilayer experimental set up.

Figure 10: Membrane formation using the droplet interface bilayer technique. a) Initially, the droplets are apart forming only the monolayers. b) Approaching the droplets leads to the spontaneous membrane formation. c) The membrane is formed, and the two droplets are separated by a contact angle 2θ.

Young's Equation: Interfacial Equilibrium

The growth of the DIB is controlled by the balance of tensions acting at the annulus, minimizing the total interfacial energy of the adhered droplets pair (Fig. 11). Surface tension is defined as the excess energy per unit area at the surface of two immiscible fluids (mJ/m^2 or mN/m). Ignoring gravitational effects, the forces acting on the membrane are the bilayer tension and the two monolayer tensions. Adding these two energy terms and minimizing the expression leads to a modified form of Young's equation (Eq.1), which predicts the contact angle between the droplets based on the interfacial tensions. These interfacial tensions are dependent on the relative favorability of interface formation as well as the area per surfactant molecule [31].

$$\gamma_b = 2\,\gamma_m\,\mathrm{Cos}\theta \qquad \text{Eq. 1}$$

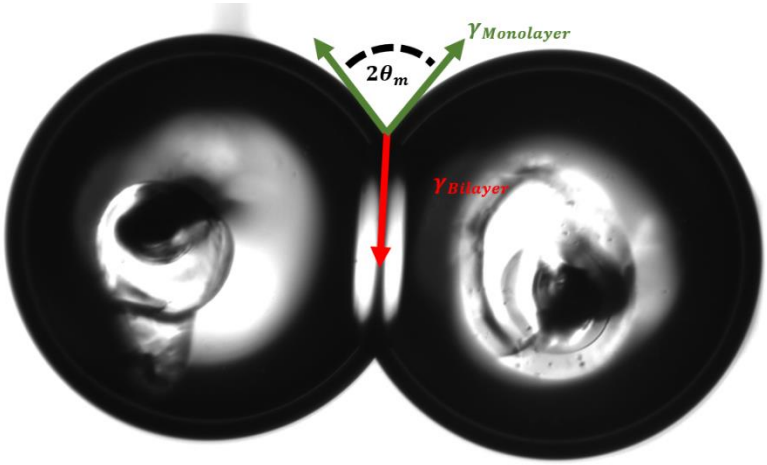

Figure 11: Interfacial tension Balance. Bilayer tension is balanced by the two monolayers separated by an angle 2θ.

The adhesion energy is an indicator of how favorable it is for the membrane to form [29]. It compares the energies associated with the bilayer tension and the two monolayer tensions. The higher the value of the adhesion energy, the more favorable the formation of the bilayer is. The adhesion energy can be seen as how much energy the system "saved" by forming the bilayer rather

than having two detached droplets per bilayer area. The equation describing the adhesion energy is the Young – Dupre equation [32], which compares the two monolayer surface tensions γ_m to the bilayer tension γ_b as follows:

$$\Delta F = 2\,\gamma_m - \gamma_b \qquad \text{Eq. 2}$$

Bilayer Electrical Model

The membrane is electrically modeled as a capacitor and a resistor in parallel [33] (Fig.12). The capacitor component arises from the impermeability of the membrane. Recall that the aqueous phase is a buffer solution, meaning that ions are present on both sides of the leaflets. Thus, it can be considered as a parallel plate capacitor having a specific dielectric permittivity governed by the hydrophobic tails of the lipids. The resistant component accounts for the imperfectness of the bilayer, or the formation of transient pores. Leaking can occur, and a resistive current can be present if there are defects in the membrane. However, having satisfactory lipids and working within the appropriate frequency range ensures having a capacitive current with negligible contribution from the resistance [1]. The magnitude of the capacitance and resistance may be linked directly to the structure and quality of the membrane, allowing for electrical investigation of membrane properties.

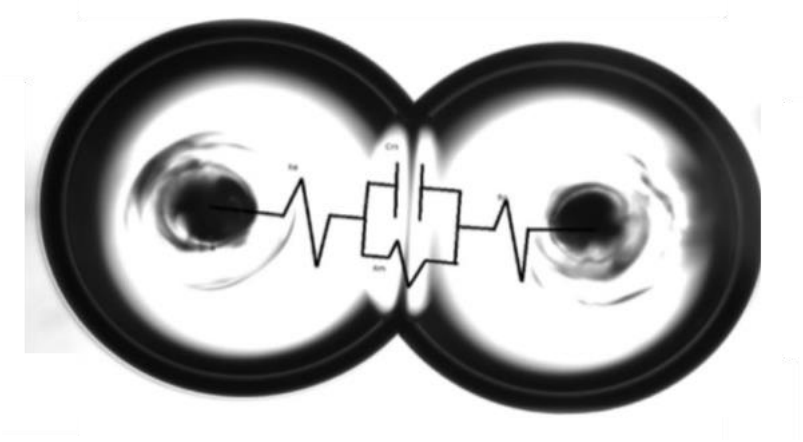

Figure 12: Electrical model of a DIB. The membrane is represented as a capacitor in parallel with a resistor, which are in series with the electrolyte resistors.

In this setup, the bilayer can be considered as a soft capacitor since the droplets are free to move under a variety of electrical or mechanical forces leading to changes in the membrane's area and thickness through electrowetting and electrocompression respectively. When a DC voltage is applied, oppositely charged sides will generate coulomb forces trying to push the leaflets closer together. Recalling the equation of a parallel plate capacitor, the total capacitance in Farad is proportional to the membrane's area and inversely proportional to its thickness as seen in Equation 3.

$$C = \frac{\varepsilon_0 \varepsilon_r}{d} A \qquad \text{Eq.3}$$

Electrowetting phenomena

Berge-Lippmann- Young Equation

Electrowetting is defined as the reduction in the interfacial tension upon the application of an electric field [34]. Similarly to a sessile droplet on a dielectric, applying a DC voltage to the bilayer leads to a reduction in the apparent bilayer tension (Fig.13). This reduction can be observed by a

relaxation in the bilayer tension as its area increases and consequently increases the contact angle between the two droplets (Fig.14, Equation (1)).

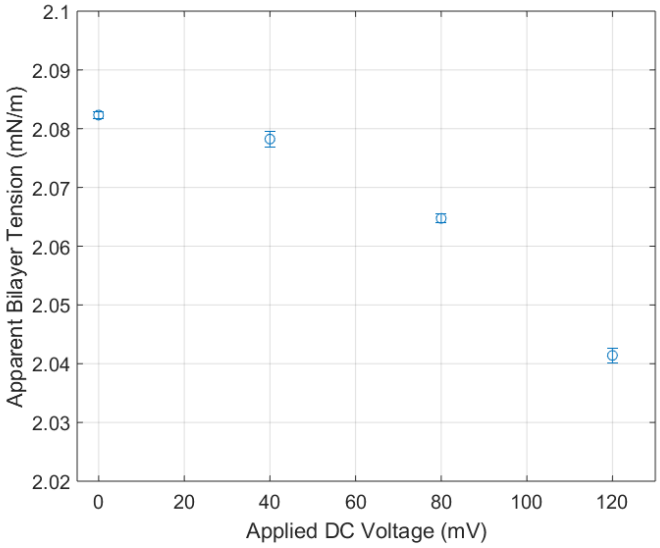

Figure 13:Reduction in the bilayer's apparent tension (mN/m) upon the application of a DC offset (mV), within a standard deviation. This data is obtained for a DIB made with DPhPC phospholipids in hexadecane oil.

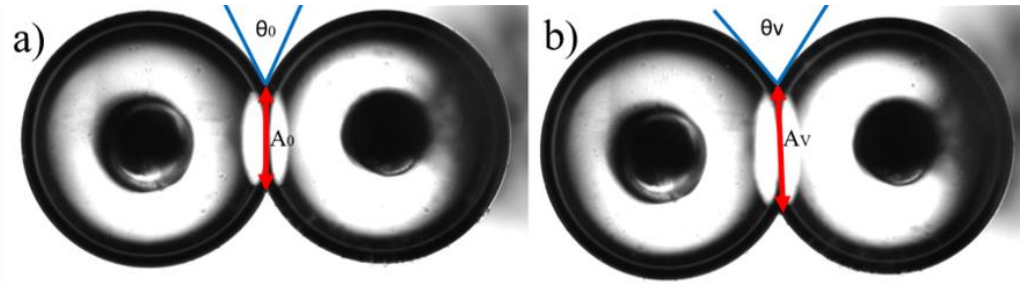

$$A_0 < A_V$$

$$\theta_0 < \theta_V$$

Figure 14: DIB under the electrowetting effect. a) With no voltage applied, the DIB has an initial area and contact angle. b) Applying an electrical field across the bilayer reduces the apparent tension, which is seen as a relaxation in the bilayer's area followed by an increase in the contact angle at the annulus.

To quantify this phenomenon, a direct relation between the applied offset and the contact angle is desired (Fig. 15). Adding the energy associated with the electric field to the total energy of the system and again minimizing the expression, the Berge-Lippmann-Young (BLY) equation specific for DIBs [35] arises:

$$\mathrm{Cos}\,\theta_0 - \mathrm{Cos}\theta_V = \frac{C_m}{4\,\gamma_m} V^2 \qquad \text{Eq. 4,}$$

where C_m is the membrane's specific capacitance i.e. capacitance per unit area ($\mu F/cm^2$) and θ_V is the contact angle with an applied voltage. Note that this equation assumes the membrane is incompressible and maintains a constant thickness.

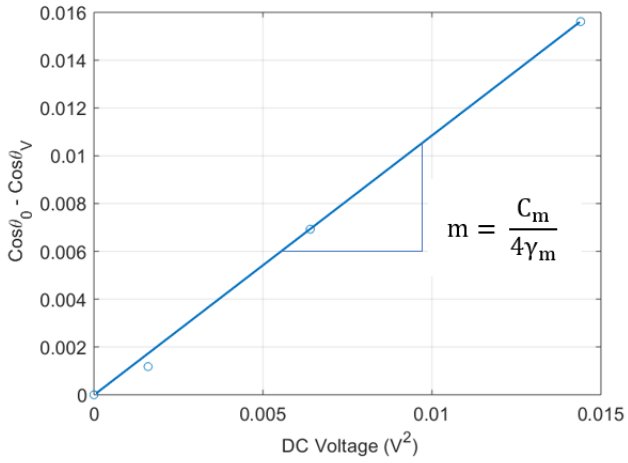

Figure 15: Change in the contact angle as a function of the square of the voltage applied. The slope of the line depends on the membrane's specific capacitance and the monolayer tension.

Quadratic Behavior

Another interesting observation for the electrowetting phenomena with DIBs is the quadratic behavior of the total capacitance and membrane area with respect to the voltage (Fig. 16). This behavior is empirical, but it has been seen and discussed in the literature [36-38], where the following equations were observed:

$$C = C_0(1 + aV^2) \qquad \text{Eq.5}$$

$$A = A_0(1 + bV^2) \qquad \text{Eq.6}$$

$$C_m = C_{m_0}(1 + \beta V^2) \qquad \text{Eq. 7}$$

the zero subscript indicates the value with no electrical field applied; a, b and β are defined as the electro-compression coefficients. Note that when no electrical field is applied, i.e. V=0, the value is at its initial minimum as seen in Figure 16.

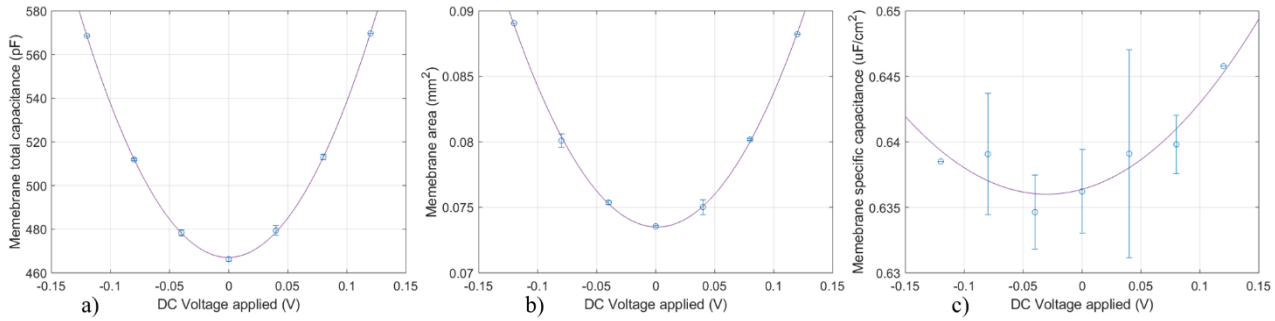

Figure 16: Quadratic behavior with voltage for a) the total Capacitance in pF, b) bilayer area in mm^2 and c) membrane's specific capacitance, for a DPhPC- Hexadecane membrane.

One can directly notice that the specific capacitance's behavior is different than the previous equations. In fact, the membrane's specific capacitance change with voltage is difficult to quantify. Since the membrane is a soft capacitor, electro-compression or membrane thinning occurs due to coulomb forces as the result of the application of a DC voltage [39]. A reduction in the membrane's dielectric thickness is reflected by an increase in its specific capacitance (Eq. 3). However, it has been seen to vary significantly from one DIB to another as it can show none, minor or significant changes (Fig. 17). This can be mainly related back to the type of oil used. Low chain-length oils, such as dodecane and tetradecane, form thicker lipid bilayers [36] as oil molecules often remain between the two leaflets. Thus, the reduction in the membrane's thickness, in this case during

electrocompression, is linked to the expulsion of oil from between the leaflets. Higher chain oils lead to thinner membranes i.e. solvent free bilayers, that usually show no or slight compression with voltage [40].

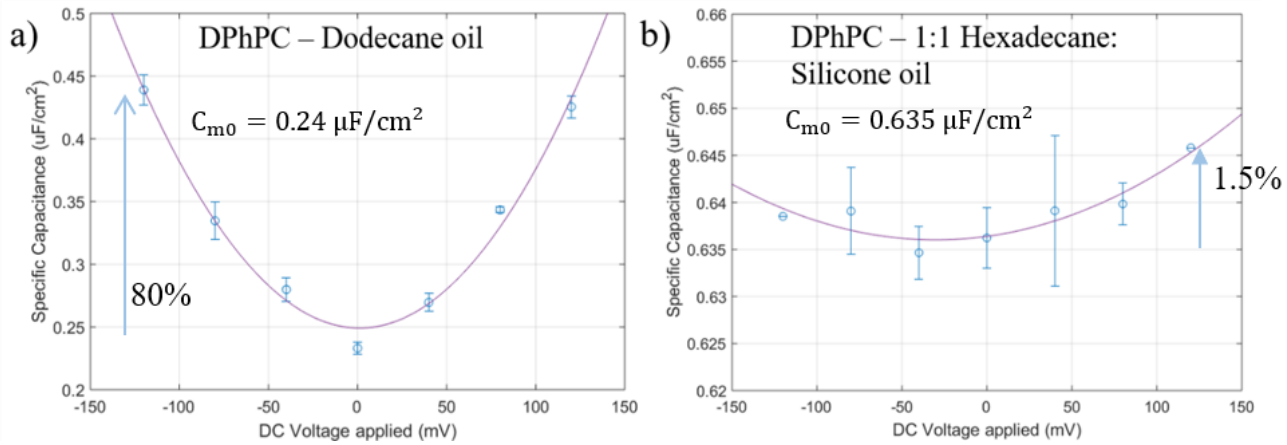

Figure 17: Electrocompression of membranes made with a) Dodecane oil – lower chain oil – b) Hexadecane and silicone oil – higher chain oil. Note the specific capacitance at equilibrium, and the magnitude of the change during electrocompression.

Chapter 3: Asymmetric DIBs

One of the main advantages of DIBs is its ability to form asymmetric membranes in the simplest way. To recall, a membrane is called asymmetric if it shows any unevenness between the two droplets, or leaflets. Droplets having different volumes, different type of salt dissolved, different salt concentrations, different phospholipids or any other dissimilarity form asymmetric membranes [41]. These membranes differ from standard symmetric membranes as they are permanently charged, meaning they have a potential offset even in the absence of any electrical field [39]. Figure 18 shows the transmembrane potential from one bulk electrolyte solution to the other. The charge distribution in the electrolyte solutions follows the Gouy-Chapman double layer theory, which describes the behavior of ions and potential near a charged surface. It predicts that the potential is exponentially changing from zero in the bulk solution, to the value of the surface charge once it reaches the surface. Within the membrane, the potential distribution is similar to a capacitor's. The difference in potential between the two electrolyte solutions is the membrane's potential offset. This offset requires a voltage equal to it in magnitude but opposite in direction to make the electrolytes potentials at the same level and neutralize the bilayer.

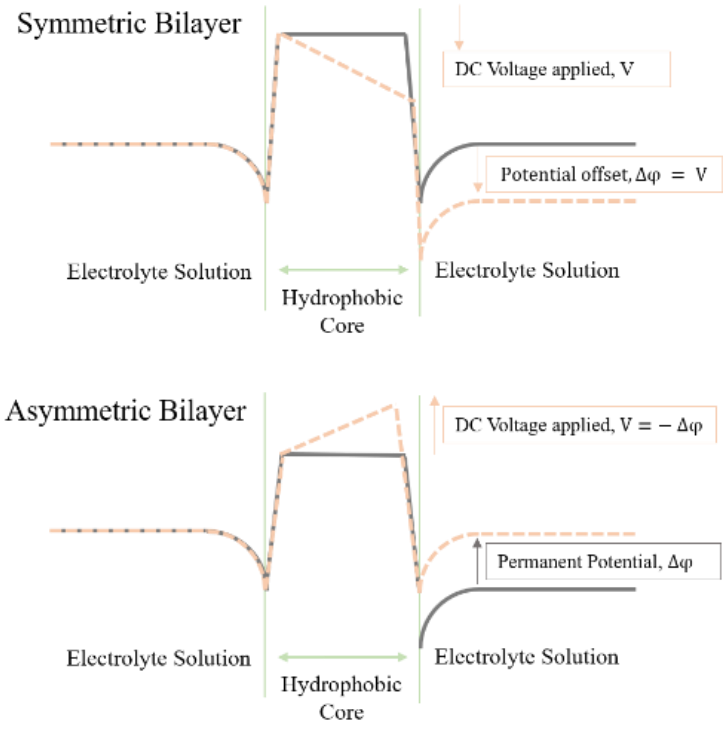

Figure 18: Transmembrane potential profile for an asymmetric bilayer.

This shift is observed via electrowetting experiments (Fig. 19). For the symmetric bilayers already discussed (Fig. 16 and 17), the parabola is centered at zero. This means that, in the absence of an electrical field, the membrane is uncharged. Whereas, asymmetric membranes show a potential offset even with no electrical field applied. A voltage equal in magnitude and opposite in charge is needed to neutralize the membrane and get the minimum capacitance. The equations describing this behavior are as follows [39]:

$$C = C_0(1 + a(V + \Delta\varphi)^2) \qquad \text{Eq. 8}$$

$$A = A_0(1 + b(V + \Delta\varphi)^2) \qquad \text{Eq. 9}$$

$$C_m = C_{m_0}(1 + \beta(V + \Delta\varphi)^2) \qquad \text{Eq. 10,}$$

where $\Delta\varphi$ is the membrane's potential offset in mV.

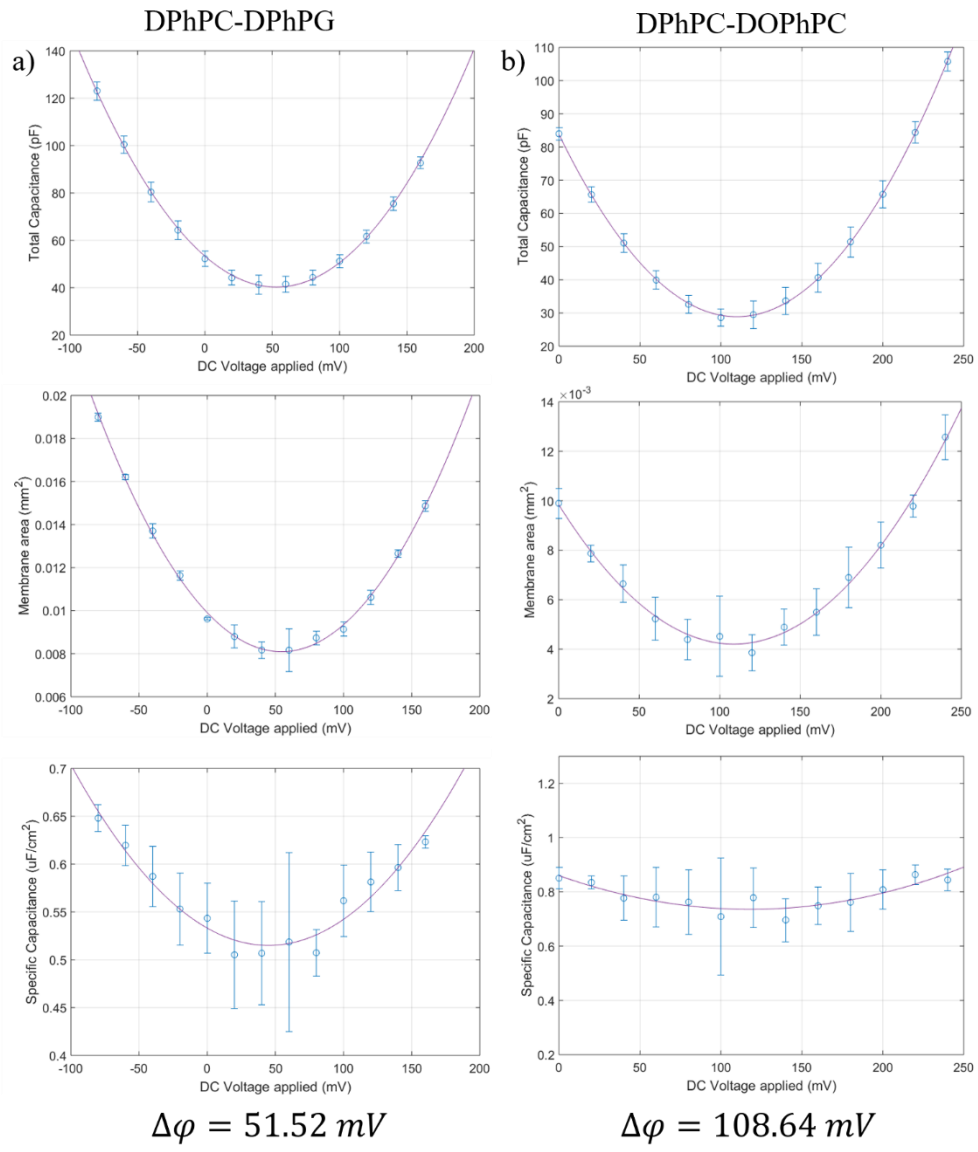

Figure 19: Quadratic behavior – total capacitance, membrane area and specific capacitance - with respect to the voltage. Membranes are formed with one droplet containing DPhPC and the other a) DPhPG, and b) DOPhPC. The oil used is tetradecane.

Chapter 4: Cholesterol – Phospholipids Interaction

Cholesterol Behavior in Lipid Monolayers: The Umbrella Effect

Cholesterol is a lipid that is naturally present in biological cells and integrates into the cell membranes at variable concentrations depending on the cell's function [42]. Cholesterol is unique in its structure as its hydrophilic head is much smaller than its bulky hydrophobic tail (Fig. 20).

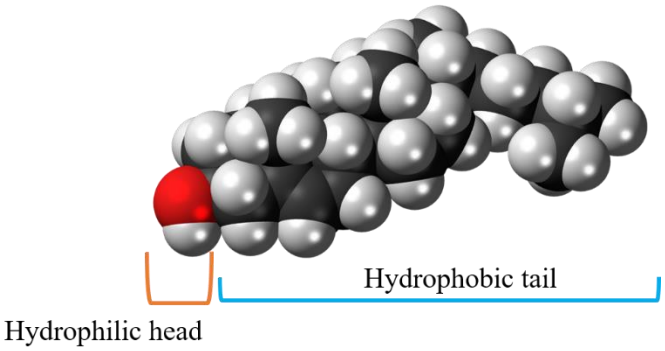

Figure 20: Cholesterol molecule. Hydrophilic head is geometrically much smaller than its hydrophobic tail [12].

In the presence of a water-oil interface, cholesterol molecules tend to merge towards the surface, but struggle to keep their hydrophobic tail from contacting water due to the ratio of the hydrophobic and hydrophilic dimensions [43]. The contact between the hydrophobic tail and water is highly undesirable and the system moves in a way to eliminate this contact. The reaction of cholesterol molecules in this situation has been described as the umbrella effect [44]. The umbrella model suggests that cholesterol's molecule attempt to squeeze themselves between the phospholipids in a way that their hydrophobic body is hidden under the phospholipids head. The profile of this behavior highly depends on the cholesterol's mole concentration (Fig. 21).

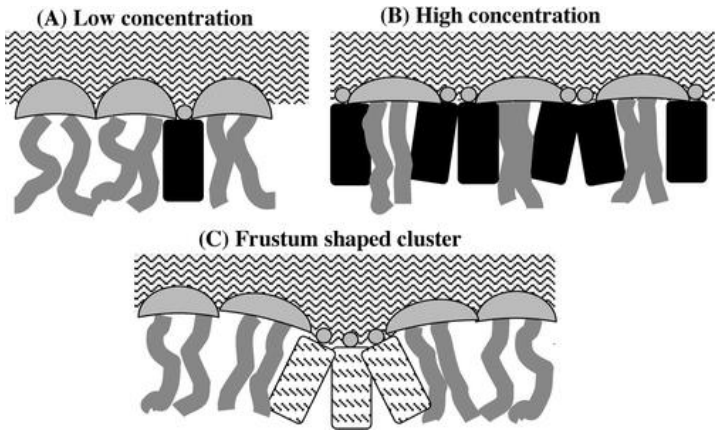

Figure 21: The umbrella model. Cholesterol's behavior in phospholipids monolayers depends on its concentration [44].

At low concentrations, cholesterol molecules can easily fit between the phospholipids. That way, cholesterol's hydrophobic tail is well covered from water by the phospholipid's head as seen in Figure 21(A). It makes sense that cholesterol finds the gaps in the monolayer and fits there, leading to the condensing effect [42]. As the concentration increases, there is less space for cholesterol molecules to hide between the phospholipids leading to the expansion of the phospholipids head. In addition, cholesterol-cholesterol interactions are highly undesirable. Thus, as the concentration increases even further, cholesterol molecules form a "frustum shaped cluster". This shape is the result of two events. One, cholesterol tails trying to minimize contact with water by assembling these clusters. Second, cholesterol-cholesterol interaction is avoided by the spread of the tails. The result is an interfacial layer that minimizes the total cost of formation but results in an inherently "frustrated" formation for the individual phospholipid and cholesterol molecules [42].

Effect of Cholesterol on Lipid Bilayers

Cholesterol modifies the lipid bilayer's properties depending on its concentration and on the type of phospholipids present. Its primary interaction is the condensing and ordering effect, which is associated with the umbrella model discussed in the previous paragraph. Cholesterol molecules

squeeze themselves between the phospholipids making the hydrophobic fatty acid tails relatively more aligned, and the membrane denser. This changes the state of the bilayer from a liquid-disordered to a liquid-ordered phase [3]. Additionally, membranes' mechanical properties have also been discussed in the literature. For instance, the area compressibility modulus has been seen to increase with cholesterol's concentration whereas the critical areal strain varies with cholesterol incorporation [45].

For unsaturated phospholipids, water permeability decreases with increasing cholesterol concentration, and this effect is emphasized as the chain length increases and unsaturation degree decreases [11]. For the case of DIBs, cholesterol has been seen to increase the monolayer and bilayer tensions [35]. Interestingly, the changes in the membrane's thickness are controversial. In some scenarios, membrane's thickness has been seen to decrease with cholesterol's increasing concentration [35, 46] and in other scenarios, the opposite was observed [9, 42]. This may be due to the formation of frustums within the membrane as the cholesterol concentration passes the threshold for their formation.

Chapter 5: Hypothesis

In this work, we propose a thorough study of the effect of cholesterol on symmetric DIBs made from DPhPC phospholipids. Membranes containing cholesterol are expected to be tougher, less permeable and more stable membranes. Few investigations have been made on the effect of cholesterol on the electro-mechanical properties of membranes made from saturated phospholipids. The DIB technique is the base of this investigation, where a set of experiments was applied on membranes showing different cholesterol concentrations. **We are mainly interested in obtaining the interfacial tensions, adhesion energy, the membrane's thickness as well as the maximum electro-compression the bilayer can withstand.** The DIB technique allows for simple investigation of all these properties through a combination of microscopy and electrical interrogation.

Chapter 6: Methodologies

Solution Preparation

In this study, the lipids-in method was used where lipids were dissolved in the aqueous phase i.e. the electrolyte solution [30]. To prepare the lipid solutions, a buffer solution was made with 500 mM of KCl and 10 mM of MOPS. For solutions containing only DPhPC, phospholipids were directly mixed with the buffer to obtain the desired concentration of 2.5 mg/mL. Six freeze-thaw cycles are necessary as well as filtering through extrusion to assure an even distribution of liposome sizes. For solutions containing cholesterol, DPhPC and cholesterol were each dissolved in chloroform and precise volumes were mixed depending on the mole fraction desired. After mixing the two volumes in a vial, argon gas was used to evaporate the chloroform and the vial was placed in vacuum for several hours to insure total evaporation of chloroform. The lipids were then hydrated with the buffer solution and stored in the freezer. Prior to using the solution and since filtering may block cholesterol molecules, sonication is a must. The aqueous solutions would be sonicated for hours until it looks clear and used directly afterwards [35]. Hexadecane was used as the oil phase, as it has shown to handle stable bilayers and its molecule is relatively large to assume a solvent-free membrane [36].

Monolayer Tension Measurements

The monolayer tension was measured using the pendant drop technique, which relies on the equilibrium between the surface tension and the gravitational force. When a droplet is suspended vertically, surface tension acts upwards on the droplet trying to minimize its surface area and maintaining its spherical shape, while gravity pulls it downwards (Fig. 22).

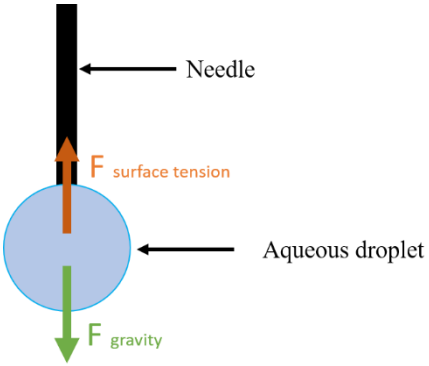

Figure 22:Surface tension and gravitational forces acting oppositely on a droplet suspended from a needle. Equilibrium between these forces enables the measurement of the surface tension.

The experimental set up consists of an aqueous droplet suspended from a needle inside a cuvette containing the desired oil (Fig. 23). Once the droplet is pushed from the needle, phospholipids and cholesterol molecules migrate towards the water-oil interface forming the monolayer, thus reducing the surface tension. This phenomenon can be observed by monitoring the droplet's shape that sags from a perfect sphere, where the surface tension is at its highest, to a pendant shape where the gravitational force and the monolayer tension are in balance (Fig. 24). The "bulb-like" shape is an indicator of a well-balanced droplet and the monolayer tension is most accurately measured.

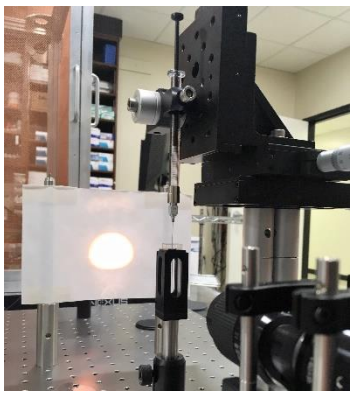

Figure 23:Experimental set up in the lab used for the monolayer tension measurements. Light, droplet and camera are horizontally aligned to obtain a 2D image of the droplet, used to estimate droplet's volume, area, curvatures and thus the interfacial tension.

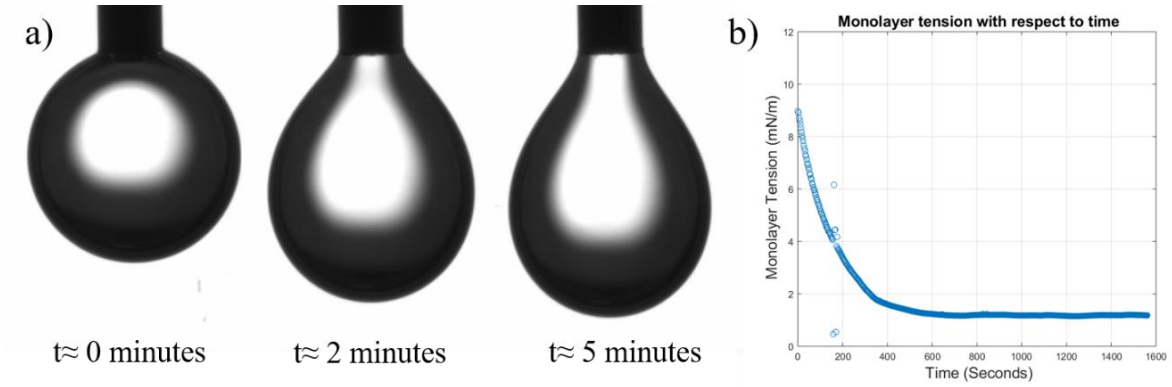

Figure 24: Pendant drop technique for monolayer tension measurements. a) The water droplet sags from a perfect sphere to a pendant shape indicating the balance between surface tension and gravitational force. b) Surface tension decreases with respect to time as the lipids reach the water-oil interface.

Recording this geometrical transformation and considering the densities of the immiscible fluids, the monolayer tension is calculated using Young-Laplace equation (Eq. 11) [47]. An accurate measurement can be ensured when Worthington number (Eq. 12), which is a dimensionless number comparing surface tension to gravity, is higher than 0.6.

$$\Delta P_0 - \Delta\rho * g * z = \gamma_m * \left(\frac{1}{R_1} + \frac{1}{R_2}\right) \qquad \text{Eq. 11}$$

$$Wo = \frac{\text{gravitational force}}{\text{surface tension force}} = \frac{\Delta\rho\, g\, V_d}{\pi\, \gamma_m\, D_n} \qquad \text{Eq. 12'}$$

where V_d denotes the volume of the droplet (μL) and D_n is the outer diameter of the needle used (mm).

Specific Capacitance and Bilayer Thickness

As declared earlier, the specific capacitance of the membrane is one of its most influential properties. Specific capacitance denotes the capacitance of the bilayer per unit area, usually expressed in $\mu F/cm^2$. The way to calculate this property is explicit, as the capacitance can be plotted with respect to the area and the slope of the straight line is the membrane's specific

capacitance. During this experiment, the membrane's capacitance at equilibrium is measured through an alternating voltage. This is done repeatedly as the droplets are gradually pulled apart through micromanipulators, reducing the size of the membrane. At each membrane size, the input sinusoidal voltage, the output current and the droplets images are simultaneously recorded. Sinusoidal voltage is preferred over other alternative signals as it provides a quick and easy way to calculate capacitance using the current-voltage equation of a capacitor as follows:

$$C = \frac{\|I\|}{\left\|\frac{dV}{dt}\right\|} \qquad \text{Eq. 13}$$

where

$$\left\|\frac{dV}{dt}\right\| = 2\pi * f * \|V\| \qquad \text{Eq. 14}$$

The signal used had an amplitude of 10 mV and 20 Hz frequency. This relatively low frequency insures a purely capacitive current across the bilayer [1]. The area of the bilayer is calculated as the area of a circle, which diameter is equal to the length of the droplets' overlying part (Fig. 25). The slope of the total capacitance vs. membrane area provides the specific capacitance (Fig.26).

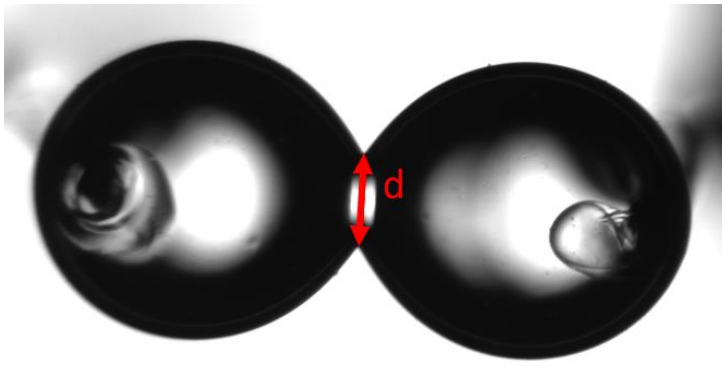

Figure 25: Droplets gradually pulled apart. The area of the bilayer is calculated as the area of a circle with a diameter "d".

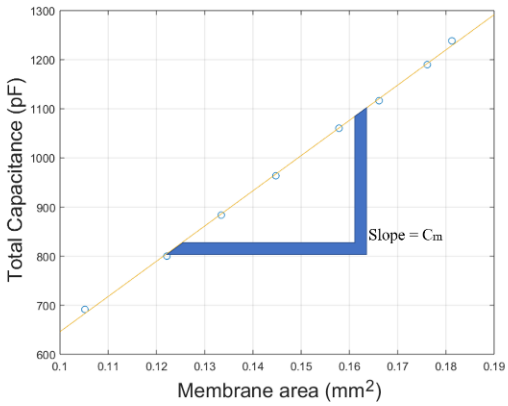

Figure 26:Membrane's total capacitance (pF) with respect to its area (mm2). The slope of the fitted line is the membrane's specific capacitance. The line must pass by zero.

The thickness of the membrane is then estimated by considering the capacitive component. Recalling the parallel plate capacitor equation, the thickness of the bilayer is obtained as shown in Equation 15, where the relative permittivity is assumed 2.2 [48].

$$d = \frac{\varepsilon_0 \varepsilon_r}{C/A} \qquad \text{Eq. 15}$$

Bilayer Tension and Adhesion Energy

To obtain the tension inside the bilayer, the contact angle between the two droplets is needed (Fig. 27). This consists of forming a DIB, waiting for its stabilization and visually estimating the contact angle using a MATLAB script. The apparent bilayer tension was calculated using Young's equation (Eq.1) and the adhesion energy using Young-Dupre (Eq.2) equation, both discussed earlier.

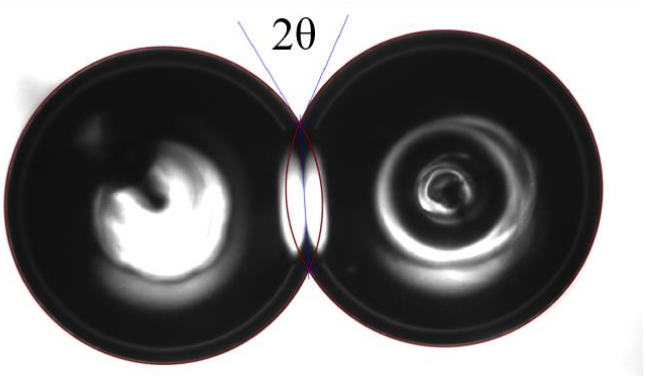

Figure 27: Image generated by a MATLAB script, showing the 2D circles that define the droplet spherical shape, and the contact angle.

Critical Dielectric Stress

In the presence of a strong electric field the droplets coalesce due to membrane failure. To obtain the maximum dielectric stress, the maximum voltage at each cholesterol concentration is needed. This experiment consists of creating a DIB, applying an AC voltage across it and slowly increasing the DC offset until the two droplets coalesce (Fig. 28 and 29).

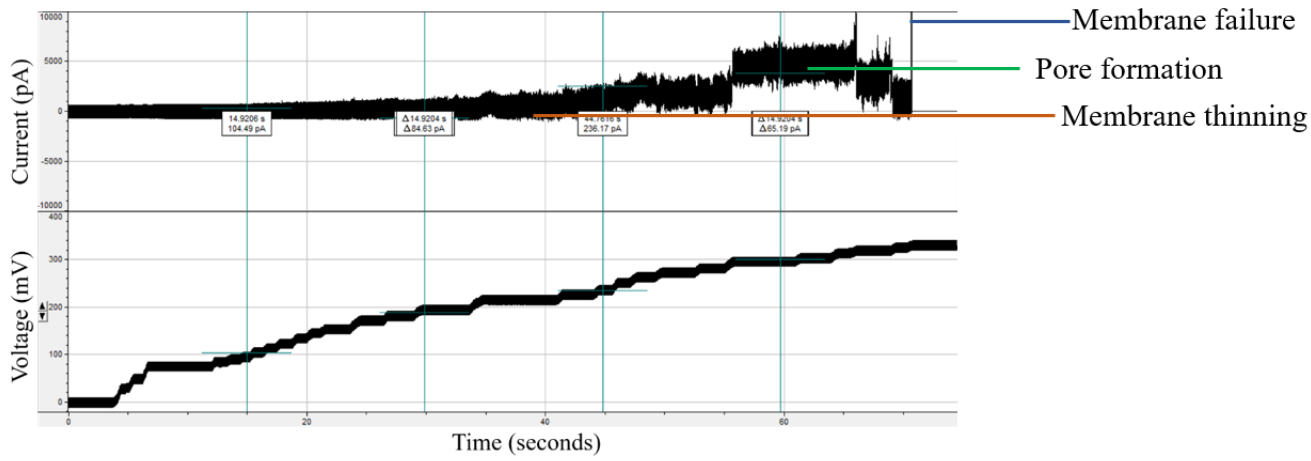

Figure 28: DC offset gradually increased with time. The increase in the current amplitude indicates bilayer thinning. The offset is an indicator of deficiencies in the bilayer leading to leak and a high resistive current until the two droplets collapse, and the current is infinity as we would have a short circuit.

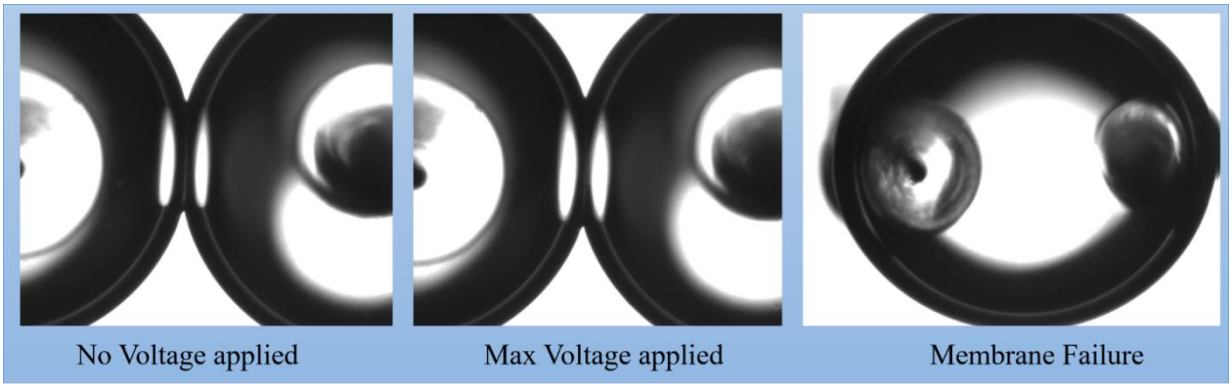

Figure 29: Microscopic images of the membrane as the DC offset increases. At first, the membrane undergoes electrowetting and electro-compression. After a certain critical voltage, deficiencies occur in the bilayer leading to failure.

Having the maximum voltage, the critical electrical field (V/μm) and critical dielectric stress (KPa) can be obtained as follows:

$$E_{max} = \frac{V_{max}}{d} \qquad \text{Eq. 16}$$

$$\sigma_{max} = \frac{\varepsilon_0 \varepsilon_r}{d^2} V_{max}^2 \qquad \text{Eq. 17}$$

Chapter 7: Results

Monolayer Surface Tension

Table 1: Surface tension of water-hexadecane with different DPhPC - cholesterol mole concentrations.

Cholesterol mole concentration	0	0.1	0.15	0.2
Monolayer Tension (mN/m)	1.139 (n=10)	1.209 (n=9)	1.273 (n=7)	1.299 (n= 6)
STDEV	0.043	0.075	0.105	0.180

Specific Capacitance and Membrane Thickness

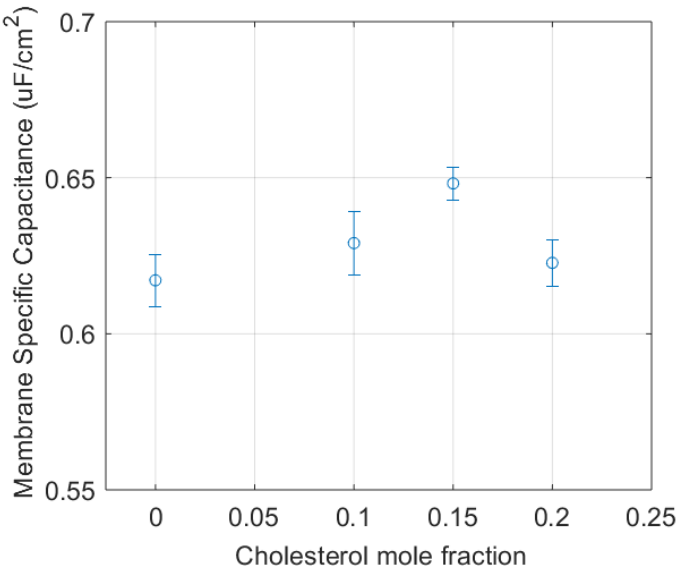

Figure 30: Average values and standard deviations of the bilayer's specific capacitance (μF/cm^2) with respect to cholesterol mole concentration.

The dielectric thickness of the membrane is directly related to the specific capacitance since the membrane is seen as a parallel plate capacitor. Using Equation 15, the thickness was obtained as follows:

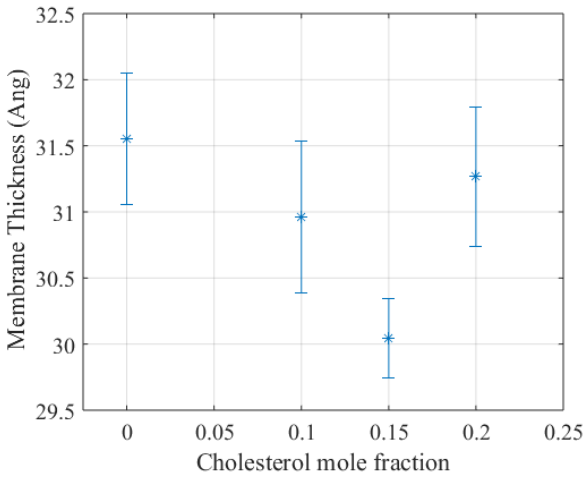

Figure 31: Average values and standard deviations of the bilayer's dielectric thickness (Angstroms) with respect to cholesterol mole concentration.

Contact Angle, Bilayer Tension and Adhesion Energy

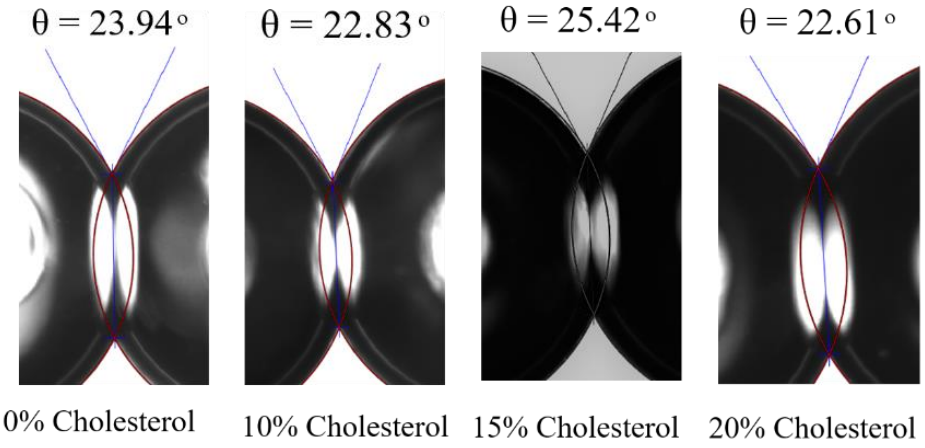

Figure 32: Average contact angle of the two droplets for different cholesterol concentration.

The bilayer tension was obtained by using Young's equation (Eq.1) and the adhesion energy from Young-Dupre (Eq.2), leading to the following results:

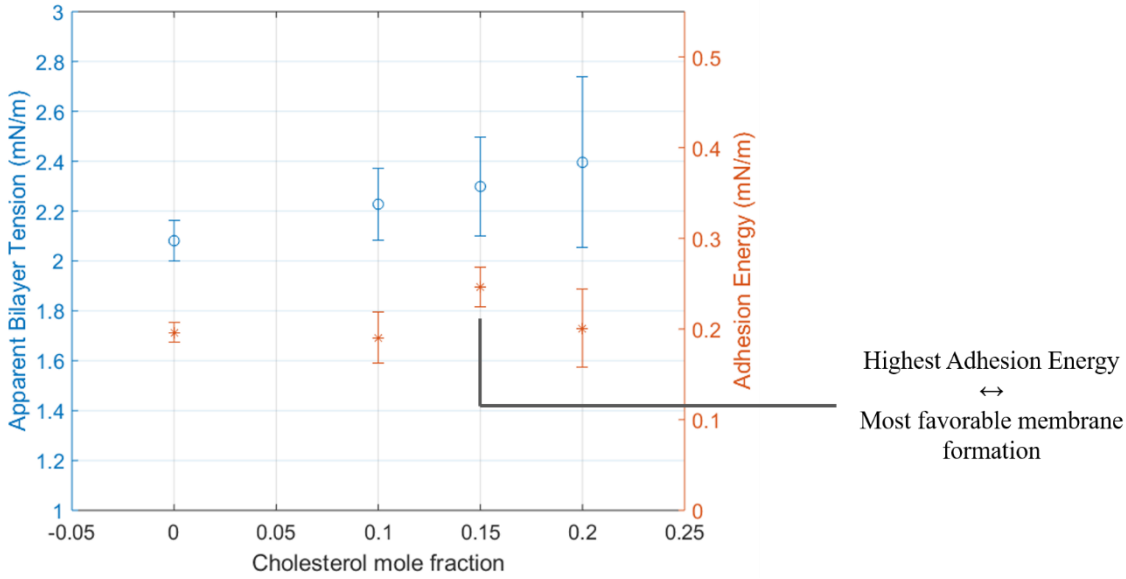

Figure 33: Average values and standard deviations of the apparent bilayer tension (mN/m) and adhesion energy per unit area (mN/m) for bilayers with various cholesterol mole fractions.

Maximum Electro-compression

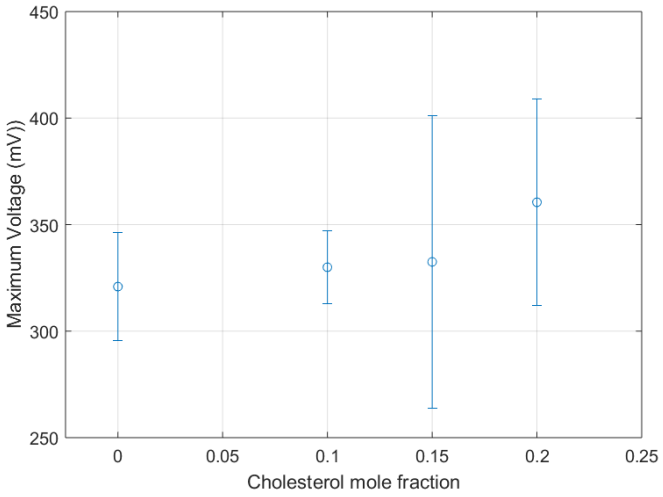

Figure 34: Average values and standard deviations of the maximum voltage (mV) the membrane was able to withstand with respect to the cholesterol concentration.

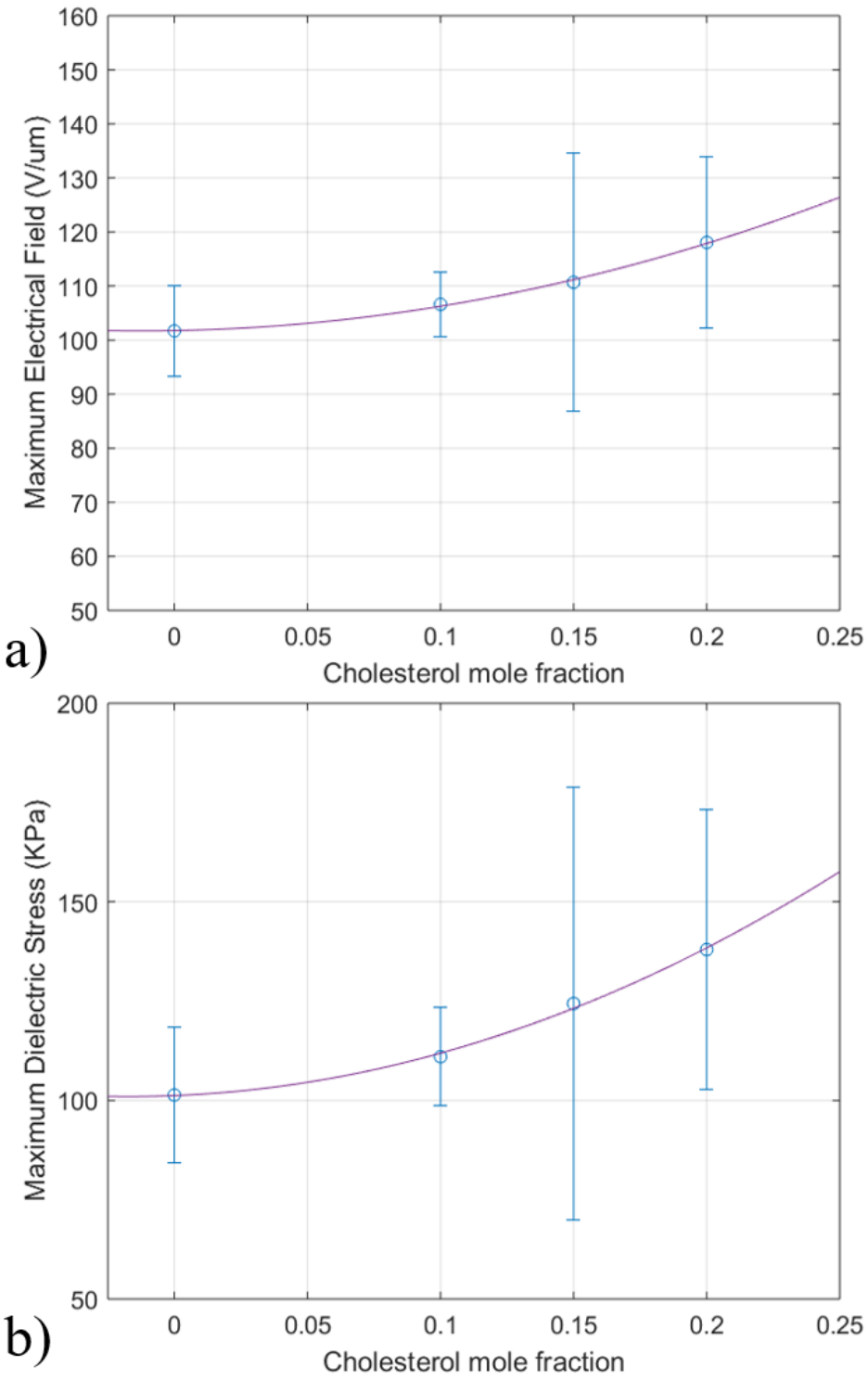

Figure 35: a) Average values and standard deviations of the critical electrical field (V/μm) and b) critical dielectric stress (KPa) with respect to the cholesterol mole fraction.

Figure 34 illustrates the maximum voltage that the bilayer was able to withstand prior to failure. The failure of the membrane was observed by the collapsing of the two adhered droplets into one, resulting in an infinite current indicating the short circuit. The maximum voltage increased from 320.9 mV (± 25.38 mV) for 0% cholesterol to 360.49 mV (± 48.53 mV) for 20% cholesterol fraction. As for the resulting maximum dielectric stress, Figure 35 shows that it goes from 100.36 kPa (± 17.07 kPa) when no cholesterol is integrated in the bilayer to 137.96 kPa (± 35.16 kPa) for 20% cholesterol mole fraction, which is almost a 37% increase.

Chapter 8: Discussion

Cholesterol Effect on the Monolayer Surface Tension

The monolayer tension of the water-hexadecane interface increases with increasing cholesterol mole concentration (Table 1). Monolayer surface tension goes from 1.139 mN/m (±0.043 mN/m) with no cholesterol included to 1.299 mN/m (±0.180 mN/m) for 20% mole fraction. This trend is expected and matches literature [35]. This increase can have multiple factors influencing it. The first factor is the size imbalance between the hydrophobic and hydrophilic parts of the lipids used. Previous work done on phospholipids showing different tail to head ratios, showed that the bigger this ratio is, the higher the corresponding surface tension [49]. As discussed earlier, cholesterol molecule has a bulky hydrophobic tail compared to its small hydrophilic head. This geometrical imbalance seems to be reducing the cohesive forces less than geometrically proportional phospholipids. The second factor is the umbrella effect discussed earlier. Cholesterol molecules, especially at a relatively high concentration, tend to form a frustum shaped cluster (Fig. 21) at the water-oil interface. This aggregation bends the surface (Fig. 36) leading to bending tension. Bending stress is similar to interfacial stress as they are both oriented along the surface – tangential forces. Thus, the bending stress combines with the interfacial tension leading to a higher value than when only phospholipids are present. This cone shaped liked aggregation of cholesterol molecules is the result of first, undesired cholesterol-cholesterol interaction, second, undesired contact between water molecules and hydrophobic tail and third, cholesterol molecule's wedge-shaped. The last reason can be further explained in a scenario where cholesterol is dissolved in an

aqueous medium only. Due to its molecular shape, cholesterol prefers to form a micelle and not a bilayer[50].

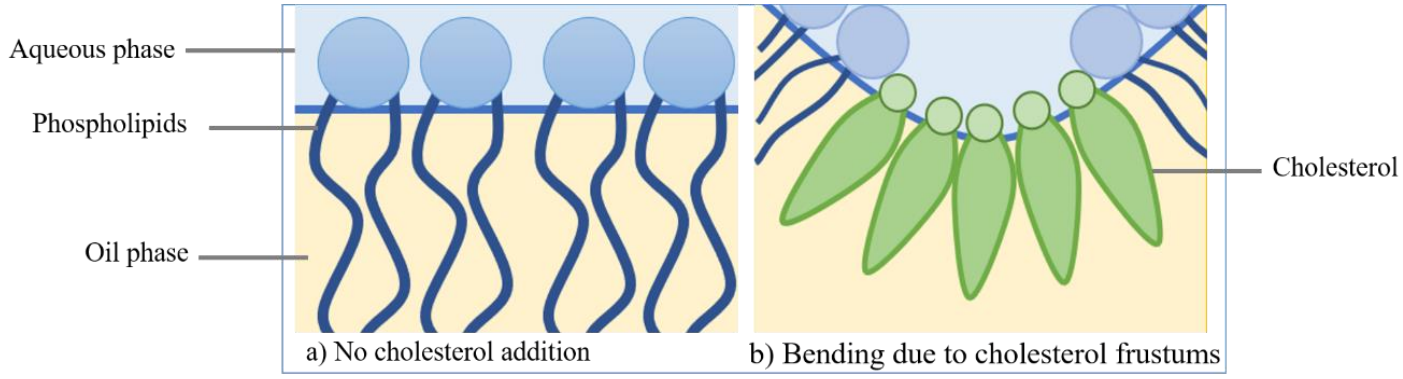

Figure 36: Water-oil interface with and without cholesterol integration. a) When only phospholipids are present, the monolayer is flat and surface tension is at its minimum. b) Cholesterol inclusion forms frustum shaped clusters, bends the surface leading to a higher interfacial tension.

Adhesion Energy, Disjoining Pressure and their correlation to Membrane Thickness

The specific capacitance increases with cholesterol concentration from 0.617 μF/cm^2 (±0.008 μF/cm^2) with no cholesterol to 0.648 μF/cm^2 (±0.005 μF/cm^2) for 15% and goes back down with 20% to 0.623 μF/cm^2 (±0.007 μF/cm^2). Thus, the membrane's thickness shows a slight reduction from 31.55 A^o (±0.499 A^o) with no cholesterol incorporation to 30.03 A^o (±0.300 A^o) for 15% cholesterol mole fraction, then moves back up to 31.26 A^o (±0.527 A^o). This change does not follow a clear trend and one can't really define cholesterol's effect on the bilayer's thickness. However, one possible explanation for membrane thinning can be the cholesterol's umbrella effect. As seen in Figure 36, cholesterol aggregation causes surface bending and since the hydrophobic part forms the inner layer of the membrane, bending of the surface is expected to reduce the bilayer's geometrical thickness. The noticeable thickening for 20% mole fraction could

be explained by the idea that there is a concentration threshold for frustums formation, after which the cholesterol tends to form micelles in water and do not integrate into the bilayer.

The adhesion energy is the energy that the system "saves" by forming the bilayer rather than having the two droplets separate. It is an indicator of how favorable it is for the membrane to form. Results show that the adhesion energies for 0, 0.1, and 0.2 cholesterol mole fraction are almost similar with an average value of ≈ 0.195 mN/m (± 0.0042 mN/m). However, 0.15 mole fraction has shown a greater value of 0.246 mN/m (± 0.0022 mN/m), indicating that this is the most favorable cholesterol concentration for this oil – phospholipids combination.

The adhesion energy can also be discussed as the integral of the disjoining pressure over the bilayer's thickness (Eq.18).

$$\Delta F = \int_{\infty}^{h_0} \prod(h)\, dh \qquad \text{Eq.18}$$

The disjoining pressure is the summation of many attractive and repulsive forces acting simultaneously on the bilayer. All of them as a function of its thickness (Fig. 37). The most dominant forces are the attractive Van der Waals forces, repulsive steric forces and in the presence of an electric field, coulomb attractive forces are added [51]. In the DIB scenario, equilibrium is established when the disjoining pressure at the thin film equals the Laplace pressure inside the droplets. The addition of the dielectric force leads to a thinner bilayer as these attractive forces increases the total disjoining pressure at interface. Figure 38 validates the concept as the thinnest bilayer used in this work shows the highest thin film pressure – that would be for the 15% cholesterol mole fraction.

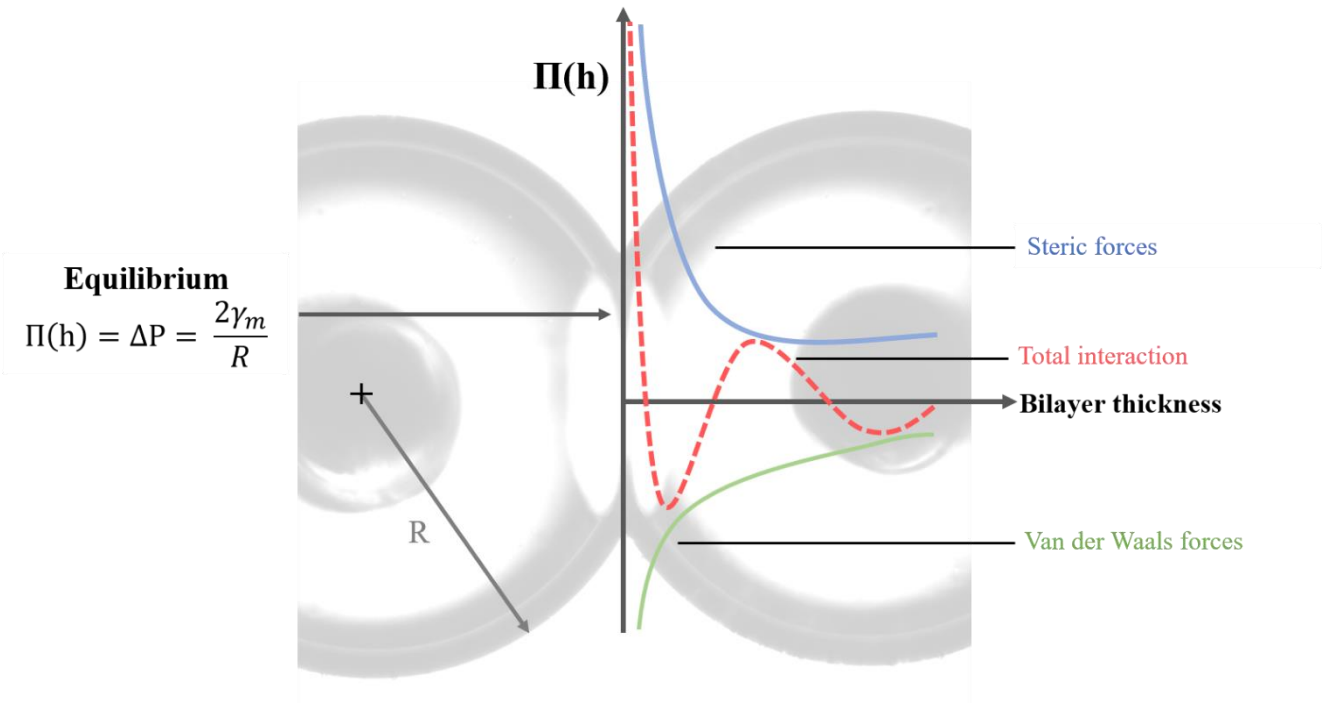

Figure 37: Representation of the disjoining pressure as a function of the bilayer thickness. The two main forces acting on the thin film are the Van der Waals attractive forces and the steric forces.

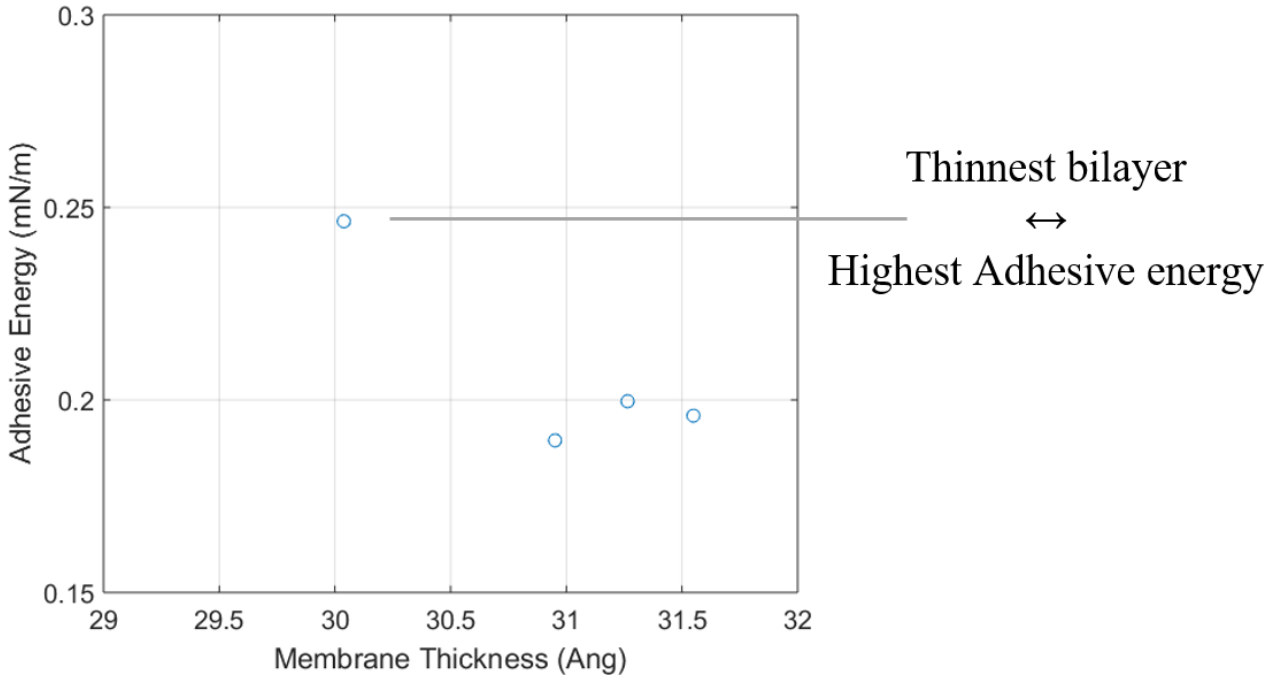

Figure 38: Membrane energy of adhesion (mN/m) as a function of its thickness (A).

Maximum Electric Field and Dielectric Stress

Upon the application of a DC voltage, membrane failure occurs when the resulting coulomb forces matches or exceeds its critical strength. Depending on its mechanical rigidity, the membrane compresses to a certain extent before failure, or the merging of the two droplets into one. Prior to total failure, and at a voltage lower than the maximum, the bilayer forms pores that are detected by an offset in the current (Fig. 28). These pores are regions in the membrane where water permeability is allowed, resulting in a significant reduction in its resistance. However, in this work, the critical voltage was defined as the voltage that causes the two droplets to merge.

As seen in Figure 35, the maximum dielectric stress the membrane can withstand goes from 100.36 kPa (± 17.07 kPa) when no cholesterol is integrated in the bilayer to 137.96 kPa (± 35.16 kPa) for 20% cholesterol mole fraction. This is almost a 37% increase. As we know of, this increase has not been recorded for DIBs before. This increase is a direct result of the ordering and condensing effect discussed earlier. Cholesterol is known to fill the gaps in between the phospholipids leading to a more sealed, packed and gel-like bilayer. In addition, DPhPC at room temperature forms bilayers that are in the liquid state [52], which makes the effect of cholesterol even more significant. Thus, cholesterol changes DPhPC bilayers from a liquid to a gel-like physical structure. This change in the bilayer's state could be increasing its compressibility modulus making it withstand higher electrical forces.

Lipids in Oil

Another set of experiments was conducted where the lipids where dissolved in oil instead of in the aqueous solution – lipids-out scenario. The concentration used were 20%, 40% and 60% cholesterol. The oil phase in this case was a 1:1 mixture of hexadecane and silicone oil. This mixture has multiple advantages. First, silicone oil has a density comparable to that of water,

making the two phases' densities closer to each other and thus minimizing the gravitational effect on the hanging droplets. Second, dissolving lipids in hexadecane and silicone oil seems to make the formation of monolayers considerably faster than if they were only dissolved in hexadecane. Note that for solutions with no cholesterol, lipids-in and lipids-out scenario gave a very similar monolayer tension with a difference in the average of 0.0073 mN/m, which is smaller than the standard deviations of both tensions. Even though different oil mixtures were used – for lipids-in only hexadecane and for lipids-out 1:1 mixture of hexadecane and silicone oil – but similar interfacial tensions were obtained indicating that silicone oil is a passive oil that does not highly influence the properties of the surface.

The lipids-out technique differed from the lipids-in technique in two ways. First, the ability to form solutions with a high cholesterol concentration. While preparing the solutions, it was much easier to create high concentrations of cholesterol when the lipids were dissolved in oil. However, a concentration higher than 20% would not properly dissolve in water. Second, the changes in surface tension for lipids-in scenario is much higher than for lipids-out even for smaller concentrations. The monolayer tension has increased from 1.123 mN/m (± 0.069 mN/m) for no cholesterol involved to 1.265 mN/m (± 0.014 mN/m) for 0.4 cholesterol mole concentration and went back down to 1.192 mN/m (± 0.008 mN/m) for 0.6 fraction (Fig. 39). Looking at the increase in tension from 0 to 20% cholesterol, it is a 2.5% increase for lipids-out whereas its almost 14% for lipids-in.

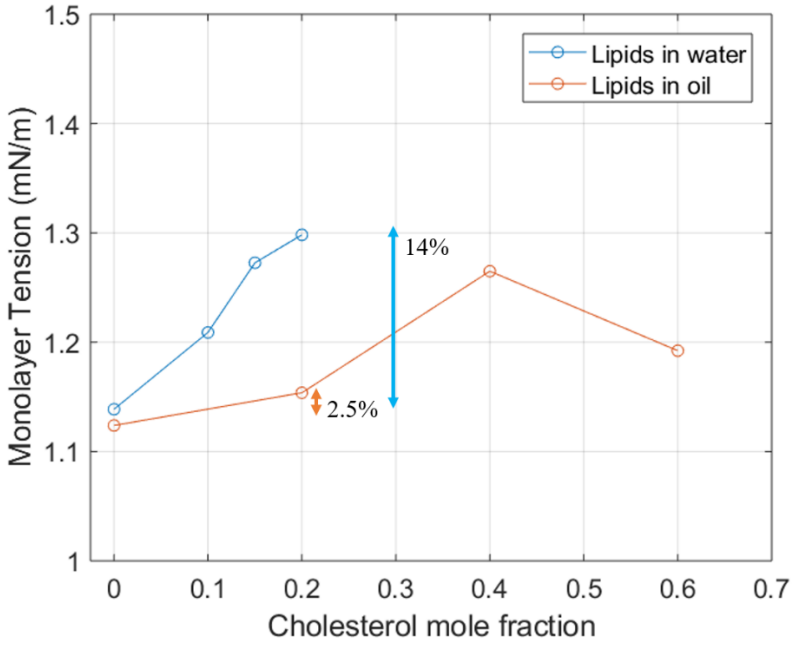

Figure 39: Monolayer tension with respect to the cholesterol fraction, for lipids dissolved in water and lipids dissolved in oil.

The simplest explanation is that cholesterol molecules favor to be in oil. It is energetically favorable to form micelles that prevents them from going into the monolayer, which explains the smaller modification in the monolayer surface tension (Fig. 40). Recall that cholesterol's hydrophilic head is much smaller than its bulky hydrophobic tail; this special geometrical form enables it to easily form micelles in an apolar medium protecting the head inside while the tails are exposed to the medium. This form is the most favorable for cholesterol molecules as it reduces the total energy of interactions [50].

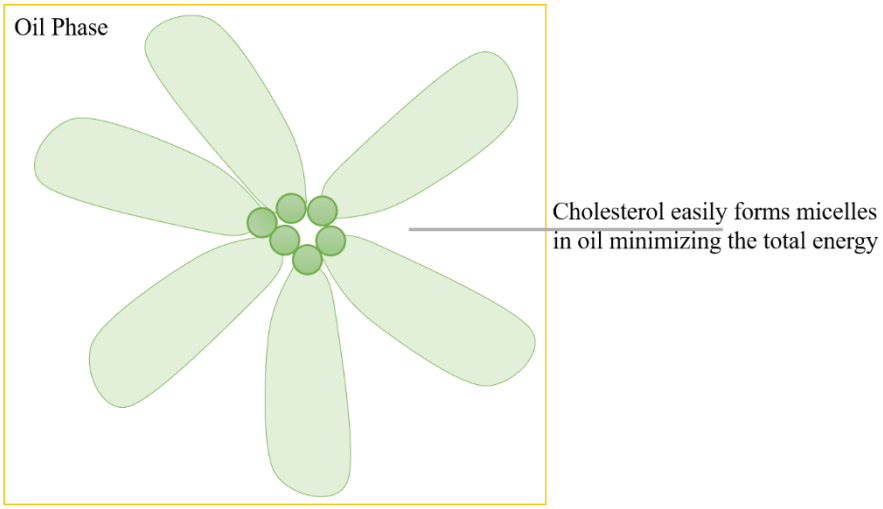

Figure 40: Cholesterol molecules forming a micelle in oil, leading to the most favorable form as it minimizes the total energy of interactions.

This analysis can be supported by a previous work done on the stability of cholesterol molecules in contact bubble bilayers [53]. There, lipid bilayers were created at the interface of two lipid-coated aqueous droplets supported by moving pipettes and submerged in oil, same concept as DIBs. Cholesterol concentrated solution was sprayed at the bilayer. Cholesterol dependent proteins were used to track the presence/absence of cholesterol in the bilayer. It was observed that whenever cholesterol molecules were ejected on the bilayers, they would quickly integrate between the leaflets, but then gradually phase back out into the bulk oil phase until no cholesterol is left in the bilayer. This experiment shows the favorability of the cholesterol molecules to be present in the apolar medium rather than in lipid membranes.

Chapter 9: Conclusion

In this work, the effect of cholesterol on the electro-mechanical properties of lipid membranes was investigated. The droplet interface bilayer technique was used as the platform for membrane formation. DIBs provide a flexible set-up for electro-mechanical characterization of lipid membranes due to their purely fluidic nature. Cholesterol is unique in its structure as it has a small hydrophilic head compared to its bulky hydrophobic tail. Cholesterol increases monolayer surface tension due to its disproportional amphiphilic ratio and/or to frustum shaped clusters that form at high cholesterol concentrations leading to an additional bending tension on the surface. Bilayer tension and the energy of adhesion were obtained, and cholesterol had an insignificant effect on the membrane's favorability to form. However, cholesterol's most dominant effect was the increase in the bilayer's critical dielectric stress. Membrane failure occurs when the applied electrical field is equal to or beyond the membrane's maximum ability to charge and compress. Cholesterol increases the bilayer's critical dielectric stress up to 37%, making it withstand an electrical field of 137.96 kPa (± 35.16 kPa). It has been concluded that cholesterol's integration into bilayers increases its ability to withstand dielectric stress without altering the favorability of its formation.

References

1. Sarles, S.A., *Physical encapsulation of interface bilayers*. 2010, Virginia Tech.
2. Freeman, E.C., *Harnessing protein transport principles for engineering applications: a computational study*. 2012, University of Pittsburgh.
3. Plesnar, E., W.K. Subczynski, and M. Pasenkiewicz-Gierula, *Saturation with cholesterol increases vertical order and smoothes the surface of the phosphatidylcholine bilayer: A molecular simulation study.* Biochimica et Biophysica Acta (BBA)-Biomembranes, 2012. **1818**(3): p. 520-529.
4. Chen, Z., et al., *Cancer Cell Membrane–Biomimetic Nanoparticles for Homologous-Targeting Dual-Modal Imaging and Photothermal Therapy.* ACS nano, 2016. **10**(11): p. 10049-10057.
5. Lodish, H. and A. Berk, *Molecular cell biology*. Vol. 3.
6. Steck, T.L., *The organization of proteins in the human red blood cell membrane: a review.* The Journal of cell biology, 1974. **62**(1): p. 1.
7. Mohandas, N. and E. Evans, *Mechanical properties of the red cell membrane in relation to molecular structure and genetic defects.* Annual review of biophysics and biomolecular structure, 1994. **23**(1): p. 787-818.
8. Heimburg, T., *Thermal biophysics of membranes*. 2008: John Wiley & Sons.
9. Pan, J., et al., *Cholesterol perturbs lipid bilayers nonuniversally.* Phys Rev Lett, 2008. **100**(19): p. 198103.

10. Engberg, O., et al., *The affinity of cholesterol for different phospholipids affects lateral segregation in bilayers.* Biophysical journal, 2016. **111**(3): p. 546-556.

11. Lopez, M., et al., *Effects of Acyl Chain Unsaturation on Activation Energy of Water Permeability Across Droplet Bilayers of Homologous Monoglycerides: Role of Cholesterol.* Langmuir, 2018.

12. Monteiro, N., et al., *Liposomes in tissue engineering and regenerative medicine.* Journal of the Royal Society Interface, 2014. **11**(101): p. 20140459.

13. Sharma, A. and U.S. Sharma, *Liposomes in drug delivery: progress and limitations.* International journal of pharmaceutics, 1997. **154**(2): p. 123-140.

14. Samad, A., Y. Sultana, and M. Aqil, *Liposomal drug delivery systems: an update review.* Current drug delivery, 2007. **4**(4): p. 297-305.

15. Bianco, A., K. Kostarelos, and M. Prato, *Applications of carbon nanotubes in drug delivery.* Current opinion in chemical biology, 2005. **9**(6): p. 674-679.

16. Mehier-Humbert, S., et al., *Plasma membrane poration induced by ultrasound exposure: implication for drug delivery.* Journal of controlled release, 2005. **104**(1): p. 213-222.

17. Maglia, G., et al., *Droplet networks with incorporated protein diodes show collective properties.* Nat Nanotechnol, 2009. **4**(7): p. 437-40.

18. Bayley, H., et al., *Droplet interface bilayers.* Mol Biosyst, 2008. **4**(12): p. 1191-208.

19. Montal, M. and P. Mueller, *Formation of bimolecular membranes from lipid monolayers and a study of their electrical properties.* Proceedings of the National Academy of Sciences, 1972. **69**(12): p. 3561-3566.

20. Nikolelis, D.P. and C.G. Siontorou, *Bilayer lipid membranes for flow injection monitoring of acetylcholine, urea, and penicillin.* Analytical chemistry, 1995. **67**(5): p. 936-944.

21. Leonenko, Z., A. Carnini, and D. Cramb, *Supported planar bilayer formation by vesicle fusion: the interaction of phospholipid vesicles with surfaces and the effect of gramicidin on bilayer properties using atomic force microscopy.* Biochimica et Biophysica Acta (BBA)-Biomembranes, 2000. **1509**(1): p. 131-147.

22. Nollert, P., H. Kiefer, and F. Jähnig, *Lipid vesicle adsorption versus formation of planar bilayers on solid surfaces.* Biophysical Journal, 1995. **69**(4): p. 1447-1455.

23. de Planque, M.R., et al. *Controlled delivery of membrane proteins to artificial lipid bilayers by nystatin–ergosterol modulated vesicle fusion*. in *IEE Proceedings-Nanobiotechnology*. 2006. IET.

24. Thompson, M., R.B. Lennox, and R. McClelland, *Structure and electrochemical properties of microfiltration filter-lipid membrane systems.* Analytical Chemistry, 1982. **54**(1): p. 76-81.

25. Thompson, J.R., et al., *Enhanced stability and fluidity in droplet on hydrogel bilayers for measuring membrane protein diffusion.* Nano letters, 2007. **7**(12): p. 3875-3878.

26. Heron, A.J., et al., *Direct detection of membrane channels from gels using water-in-oil droplet bilayers.* Journal of the American Chemical Society, 2007. **129**(51): p. 16042-16047.

27. Freeman, E.C., et al., *The mechanoelectrical response of droplet interface bilayer membranes.* Soft Matter, 2016. **12**(12): p. 3021-31.

28. Funakoshi, K., H. Suzuki, and S. Takeuchi, *Lipid bilayer formation by contacting monolayers in a microfluidic device for membrane protein analysis.* Analytical chemistry, 2006. **78**(24): p. 8169-8174.

29. Poulin, P. and J. Bibette, *Adhesion of water droplets in organic solvent.* Langmuir, 1998. **14**(22): p. 6341-6343.

30. Venkatesan, G.A., et al., *Adsorption Kinetics Dictate Monolayer Self-Assembly for Both Lipid-In and Lipid-Out Approaches to Droplet Interface Bilayer Formation.* Langmuir, 2015. **31**(47): p. 12883-93.

31. Chen, Y., C. Helm, and J. Israelachvili, *Molecular mechanisms associated with adhesion and contact angle hysteresis of monolayer surfaces.* The journal of physical chemistry, 1991. **95**(26): p. 10736-10747.

32. Schrader, M.E., *Young-dupre revisited.* Langmuir, 1995. **11**(9): p. 3585-3589.

33. Schoch, P., D.F. Sargent, and R. Schwyzer, *Capacitance and conductance as tools for the measurement of asymmetric surface potentials and energy barriers of lipid bilayer membranes.* The Journal of Membrane Biology, 1979. **46**(1): p. 71-89.

34. Chung, S.K., K. Rhee, and S.K. Cho, *Bubble actuation by electrowetting-on-dielectric (EWOD) and its applications: A review.* International Journal of Precision Engineering and Manufacturing, 2010. **11**(6): p. 991-1006.

35. Taylor, G.J., et al., *Direct in situ measurement of specific capacitance, monolayer tension, and bilayer tension in a droplet interface bilayer.* Soft Matter, 2015. **11**(38): p. 7592-605.

36. Gross, L.C., et al., *Determining membrane capacitance by dynamic control of droplet interface bilayer area.* Langmuir, 2011. **27**(23): p. 14335-42.

37. Krogmann, F., W. Monch, and H. Zappe, *Electrowetting for tunable microoptics.* Journal of Microelectromechanical Systems, 2008. **17**(6): p. 1501-1512.

38. Quilliet, C. and B. Berge, *Electrowetting: a recent outbreak.* Current Opinion in Colloid & Interface Science, 2001. **6**(1): p. 34-39.

39. Heimburg, T., *The capacitance and electromechanical coupling of lipid membranes close to transitions: the effect of electrostriction.* Biophysical journal, 2012. **103**(5): p. 918-929.

40. Makhoul-Mansour, M., et al., *Ferrofluid-Based Droplet Interface Bilayer Networks.* Langmuir, 2017. **33**(45): p. 13000-13007.

41. Kiessling, V., C. Wan, and L.K. Tamm, *Domain coupling in asymmetric lipid bilayers.* Biochimica et Biophysica Acta (BBA)-Biomembranes, 2009. **1788**(1): p. 64-71.

42. Róg, T. and I. Vattulainen, *Cholesterol, sphingolipids, and glycolipids: what do we know about their role in raft-like membranes?* Chemistry and physics of lipids, 2014. **184**: p. 82-104.

43. Dai, J., M. Alwarawrah, and J. Huang, *Instability of cholesterol clusters in lipid bilayers and the cholesterol's Umbrella effect.* J Phys Chem B, 2010. **114**(2): p. 840-8.

44. Dai, J., M. Alwarawrah, and J. Huang, *Instability of cholesterol clusters in lipid bilayers and the cholesterol's umbrella effect.* The Journal of Physical Chemistry B, 2009. **114**(2): p. 840-848.

45. Needham, D. and R.S. Nunn, *Elastic deformation and failure of lipid bilayer membranes containing cholesterol.* Biophysical Journal, 1990. **58**(4): p. 997-1009.

46. Ipsen, J.H., O.G. Mouritsen, and M. Bloom, *Relationships between lipid membrane area, hydrophobic thickness, and acyl-chain orientational order. The effects of cholesterol.* Biophysical Journal, 1990. **57**(3): p. 405-412.

47. Berry, J.D., et al., *Measurement of surface and interfacial tension using pendant drop tensiometry.* J Colloid Interface Sci, 2015. **454**: p. 226-37.

48. Valincius, G., et al., *Soluble amyloid β-oligomers affect dielectric membrane properties by bilayer insertion and domain formation: implications for cell toxicity.* Biophysical Journal, 2008. **95**(10): p. 4845-4861.

49. Yanagisawa, M., et al., *Adhesive force between paired microdroplets coated with lipid monolayers.* Soft Matter, 2013. **9**(25): p. 5891-5897.

50. Alberts, B., *Molecular biology of the cell*. 2017: Garland science.

51. Liu, Z., et al., *Droplet-based electro-coalescence for probing threshold disjoining pressure.* Lab Chip, 2015. **15**(9): p. 2018-24.

52. Husslein, T., et al., *Constant pressure and temperature molecular-dynamics simulation of the hydrated diphytanolphosphatidylcholine lipid bilayer.* The Journal of chemical physics, 1998. **109**(7): p. 2826-2832.

53. Iwamoto, M. and S. Oiki, *Membrane Perfusion of Hydrophobic Substances Around Channels Embedded in the Contact Bubble Bilayer.* Scientific reports, 2017. **7**(1): p. 6857.

Appendices

Appendix A: Area Correction Factor

The bilayer area is calculated as the area of a circle with a diameter obtained visually from microscopy. The droplets are assumed to be perfect spheres. In reality, the droplets sag due to gravity, especially with hexadecane oil, which density is 770 Kg/m^3 compared to almost 1000 Kg/m^3 for the aqueous droplets (Fig. 42). Such a difference in density will cause the droplets to sag making the area of the bilayer elliptical rather than circular, so an area correction factor is a must.

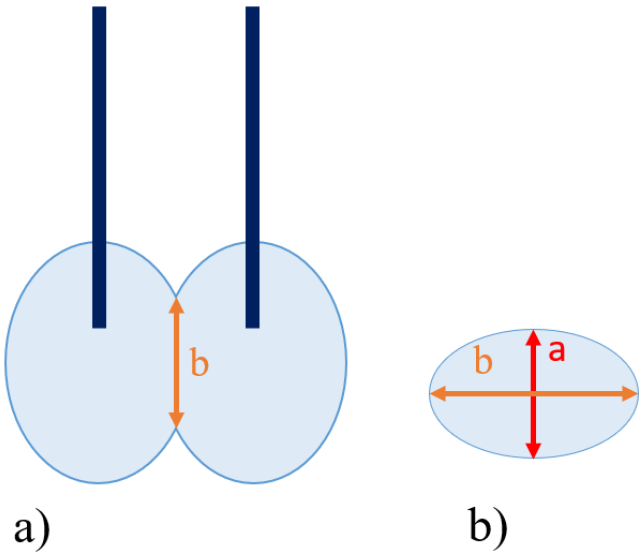

Figure 41: Actual area of the bilayer. Due to gravitation the droplets will sag from a perfect sphere and the bilayer area will be an ellipse.

An inverted microscope is used in the laboratory, so the droplets are captured from below. Thus, the diameter seen is the minor axis and the actual area is bigger than the one calculated by

MATLAB. In order to account for this effect, Graham et al estimated an area correction factor when the aqueous droplets are immersed in hexadecane oil depending on the droplets' volume (Table 2).

Table 2: Area correction factor for DIBs in hexadecane oil [35]

Droplets volume (nL)	200	300	400	500
Correction factor	1.1585	1.1773	1.2519	1.3413

Values in Table 2 were used to adjust the bilayer area and interpolation was used to obtain the correction factor for any volume in between. Note that droplets having a volume larger than 500 nL lead to weak, unstable bilayers and wouldn't adhere well to the electrodes. Whereas droplets smaller than 200 nL will lead to an undesired wetting of the electrodes as seen in Figure 43.

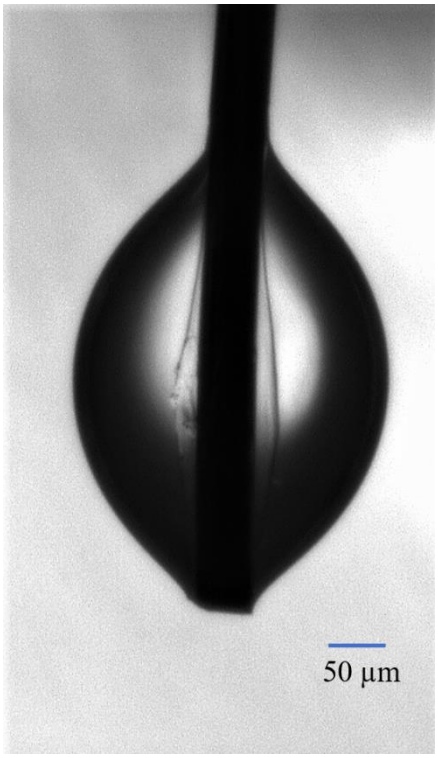

Figure 42: At small volumes, surface tension dominates gravity leading to wetting of the wire and the droplet loses its spherical shape.